WSRC-TR-2001-00499

In Situ Stress Measurements in the NPR Hole, Volume I - Results and Interpretations

by

D. Moos

Westinghouse Savannah River Company
Savannah River Site
Aiken, South Carolina 29808

M. D. Zoback

DOE Contract No. **DE-AC09-96SR18500**

This document was prepared in conjunction with work accomplished under Contract No. DE-AC09-96SR18500 with the U.S. Department of Energy

DISCLAIMER

WSRC-TR-2001-00499

FINAL REPORT

IN SITU STRESS MEASUREMENTS IN THE NPR HOLE

Volume I - Results and Interpretations

July 1992

Report Submitted to

WESTINGHOUSE SAVANNAH RIVER COMPANY

Under Subcontract No. AA00915P

by

SCIENCE APPLICATIONS INTERNATIONAL CORPORATION
360 Bay Street, New South Building, Suite 200
Augusta, GA 30901

In Situ Stress Measurements in the NPR Hole, Savannah River Site, South Carolina: Final Report to Westinghouse Savannah River Company

July, 1992

Volume I - Results and Interpretations

Prepared by
Daniel Moos
Mark David Zoback

NOTICE

Executive Summary

This report presents the results of an investigation of the magnitudes and orientations of the in situ stresses in basement rocks beneath the Savannah River Site. Stress magnitudes were measured using the hydraulic fracturing technique. Stress orientations were obtained from the orientation of stress-induced wellbore breakouts and hydraulically-induced fractures. The measurements reported here were carried out in the NPR hole, drilled to a total depth of 4000 feet near the center of the Savannah River Site, at roughly the location of the proposed New Production Reactor. The results obtained in this study are compared to previous stress measurements made using the same techniques in a series of shallower holes on the SRS, and discussed in the context of the regional stress field and potential seismic hazard.

Stresses at very shallow depth beneath the Savannah River Site are highly compressive and close to the limit constrained by the frictional strength of well-oriented reverse faults. Similar to many other sites around the world where high horizontal compression has been measured near the surface, we found that stresses in the NPR hole increase quite slowly with depth, and below about 2100 feet the magnitude of the maximum principal stress is well below that required to cause reverse faulting.

Overall, a NE-oriented direction of maximum horizontal stress was found in the NPR hole, sub-parallel to the NE-striking Pen Branch Fault. We interpret these results to indicate that potentially damaging reverse and strike-slip faulting earthquakes are unlikely to occur along the Pen Branch. For example, to the depth of ~2100' where reverse-faulting stress magnitudes were found, the S_{Hmax} direction (as measured in both the NPR hole and in shallow holes elsewhere on the SRS) is N50-70°E, almost exactly parallel to the strike of the Pen Branch, thus indicating that reverse faulting on the Pen Branch is essentially impossible. The orientation of maximum stress in the deeper part of the NPR hole (between 3000' and 3700') is ~N33°E, a distinctly more northerly direction of S_{Hmax} than shallower measurements. This orientation and the magnitudes of the horizontal stresses suggest the possibility of small, left-lateral strike-slip events along faults sub-parallel to the Pen Branch within this depth interval, as characterized by a small (M≈2.6) earthquake which occurred at about 1 km depth beneath the SRS in 1985. However, wellbore breakouts near the very bottom of the NPR Hole (3700'-4000') show a clockwise rotation implying that the ~N33°E average direction may be a consequence of a local perturbation of the stress field and is therefore not indicative of stress orientations at greater depth.

Volume I

Results and Interpretations

This is the first of two volumes summarizing the results of the stress measurement program conducted during March of 1992 at the Savannah River Plant. The principal results and data interpretation are summarized and discussed in this volume. A companion volume contains Appendices including calibration documentation and Quality Assurance forms, and presents the primary data, analyses and intermediate results. The Task Manual for Task 11 of Contract AA00915P, *In situ stress measurements at the Savannah River Site* [SAIC, 1991] describes in detail the methodology and analysis techniques used in the study, and is made part of this Report by reference.

Table of Contents

Introduction

As part of a study of seismic hazard conducted on behalf of Westinghouse Savannah River Company, in situ stress measurements were made during the spring of 1992 in a 4000-ft deep well drilled near the site of the proposed New Production Reactor (NPR). The purpose of the measurement program was to determine the magnitudes and orientations of the principal stresses beneath the plant and to extend to greater depth a suite of similar measurements conducted during the summer of 1988. This report presents the results of the stress measurement program, and discusses these results briefly in the context of local and regional geology and tectonics. We also outline the measurement program and present in appendices the primary data, intermediate results, and the records of calibrations of the critical test equipment and validations of the analysis methods.

The Savannah River Site (SRS) lies along the Savannah River about 35 km SE of Augusta, Georgia, in the Atlantic Coastal Plain (Figure 1). Coastal Plain sediments of upper Cretaceous and younger ages are exposed everywhere on the plant, and extend to an average depth of 800 to 1200 feet. Basement rocks include Triassic sandstones and mudstones of the Newark Group and Paleozoic and Precambrian age metamorphic rock of the Charlotte and slate belt groups. The basement surface dips gently (9 m per km) to the SE and strikes N62°E. Based on core results, schistosity within the crystalline basement dips uniformly about 55 degrees to the east. Triassic sands and mudstones lie within the narrow (~15 km wide) northeast trending Dunbarton basin. The Pen Branch Fault, which forms the northwest margin of the basin, cuts across the SRS, as shown in Figure 1 [see also Marine and Siple, 1974]. Seismic reflection surveys have delineated a series of faults within the basin and surrounding basement with trends roughly ENE-WSW, which include the basin bounding fault. Along these faults some reverse displacement has been observed in recent seismic surveys; the displacement apparently decreases toward the surface. None of the faults within the basin apparently penetrates the surface sediments, suggesting that motion along these faults predates Cretaceous time.

The Atlantic Coastal Plain province is within a broad region of the eastern United States characterized by a fairly consistent NE-SW direction of maximum horizontal compressive stress, as illustrated in Figure 2 [Zoback and Zoback, 1991]. This province is defined by focal mechanisms of recent earthquakes, young geologic indicators, and direct measurements of in situ stress. Figure 3 (also from Zoback and Zoback [1991]) shows determinations of the maximum horizontal stress direction within the eastern portion of North America, including the immediate region of the SRS. Earthquake focal mechanism

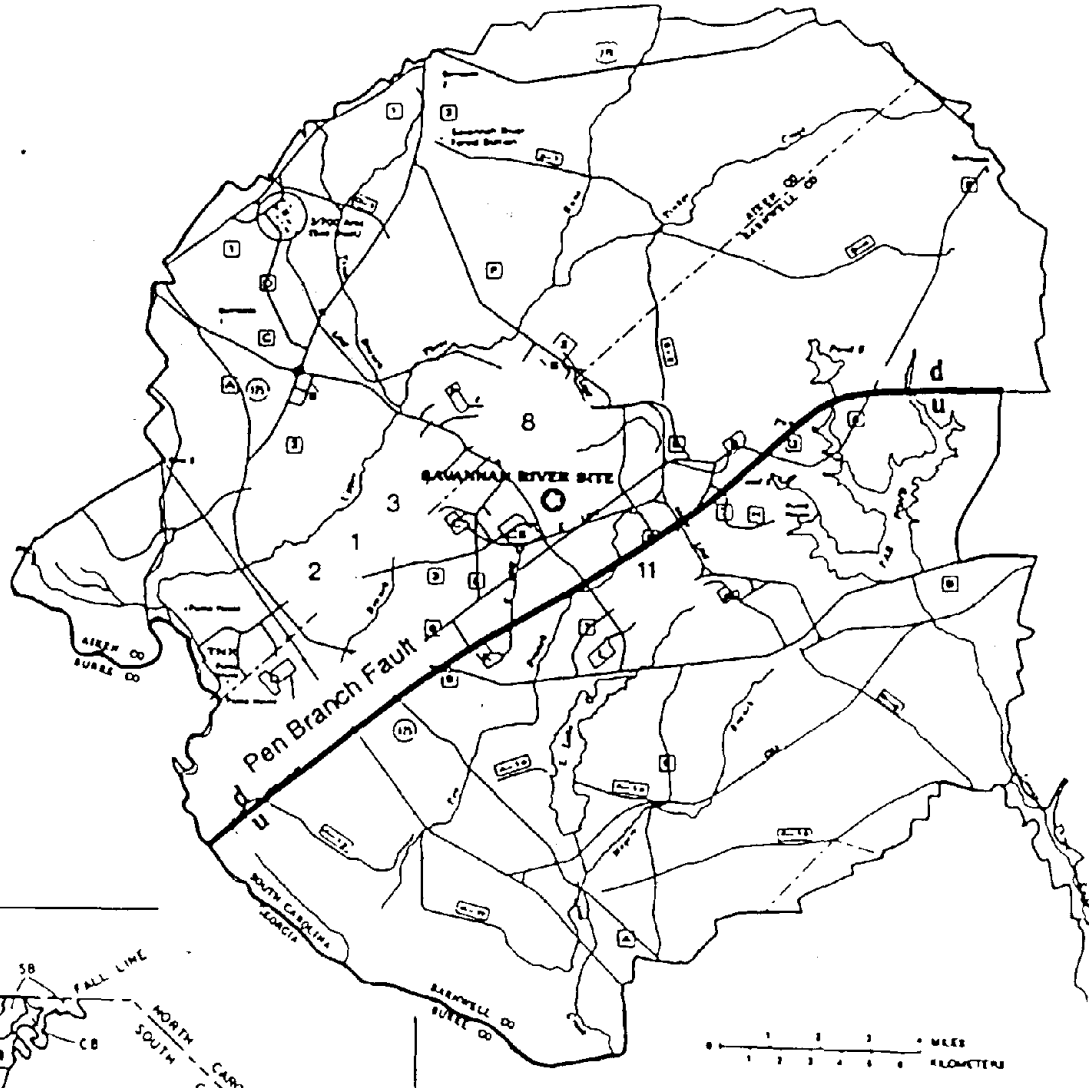

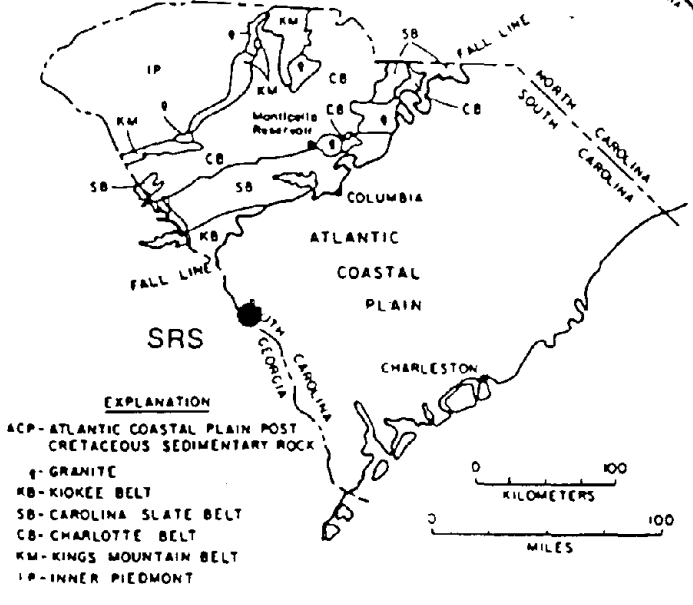

Figure 1 Geologic map of South Carolina, showing the location of the Savannah River Site (SRS) along the Savannah River southeast of Augusta, GA. Also shown is a map of the SRS showing the locations of the boreholes mentioned in this report. Numbers refer to SSW-1, SSW-2, SSW-3, DRB-8 and DRB-11 previously studied; the star shows the location of the NPR Hole. The approximate location of the NE-SW trending Pen Branch Fault, which bounds the Dunbarton Basin along its NW edge, is shown by the dark line (u on upthrown side of fault).

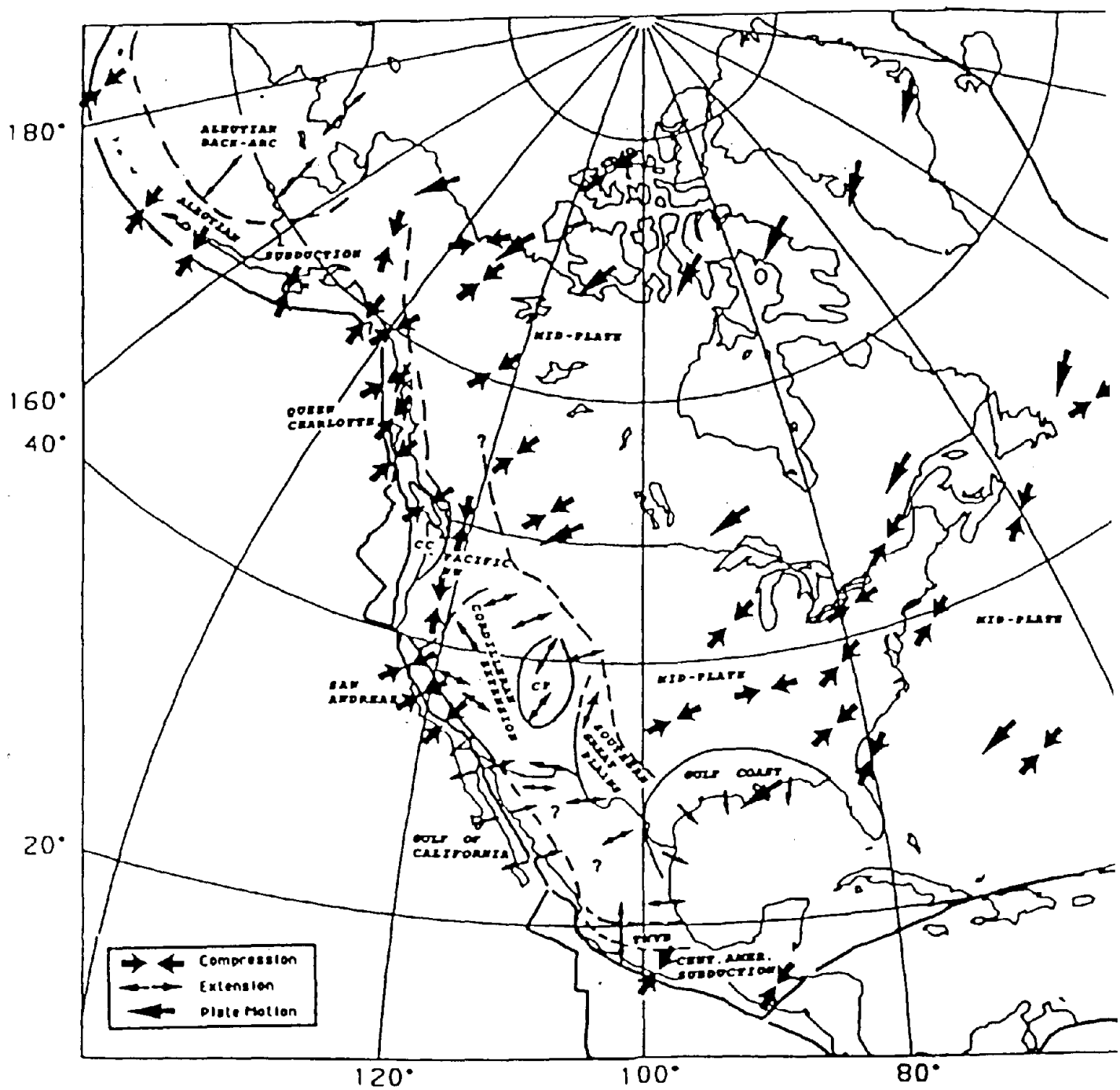

Figure 2 Stress map of North America (after Zoback and Zoback [1991]). The Savannah River Site lies within a broad zone of NE-SW compression which covers most of the eastern United States. Also shown is the direction of plate motion of the North American Plate, which is approximately parallel to the maximum horizontal compression direction, as expected for a ridge push source of intraplate stress.

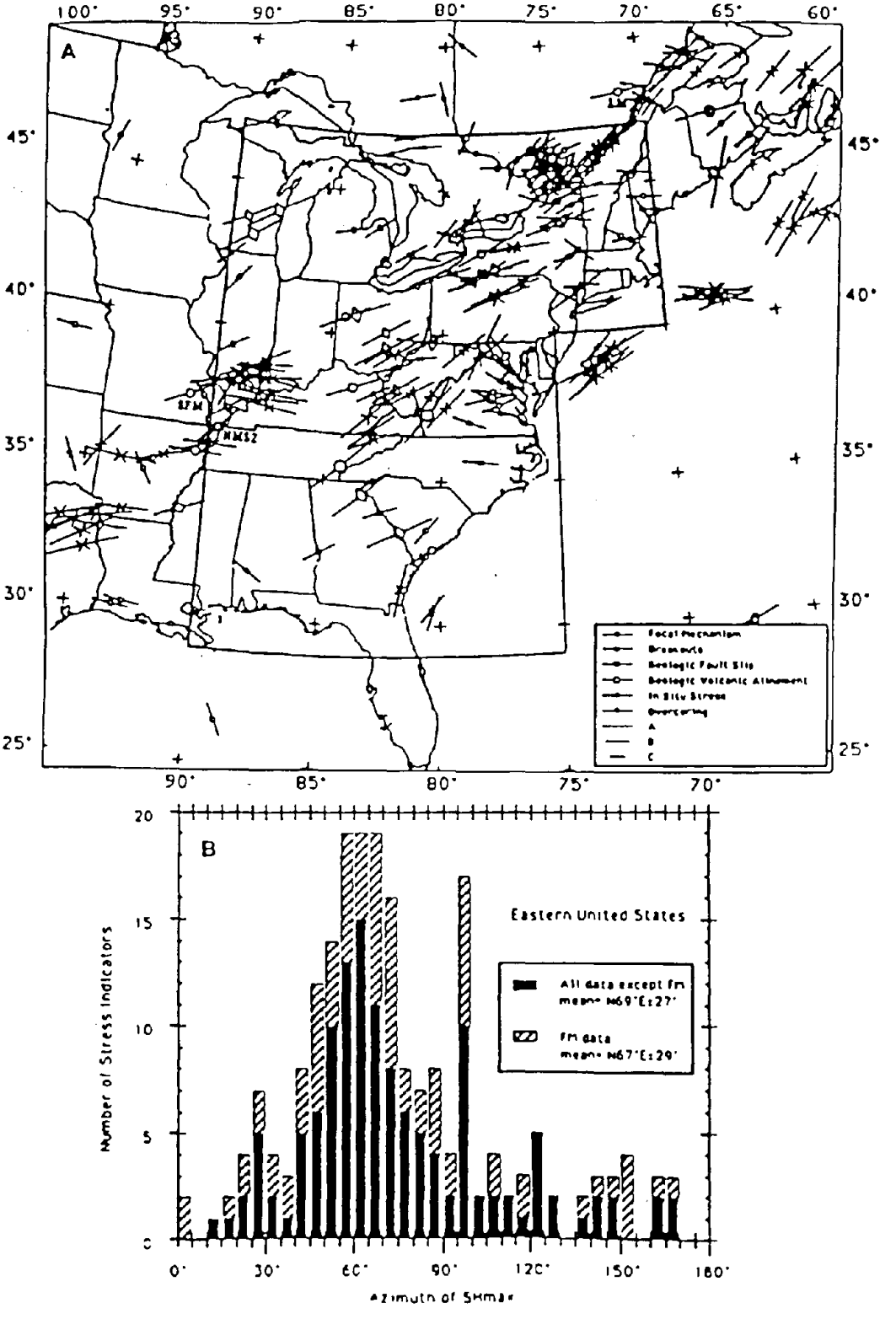

Figure 3 Stress determinations for the eastern half of North America (after Zoback and Zoback [1991]). Data points enclosed by the polygon on the map (a) are shown in the histogram (b) below comparing relatively shallow in situ stress indicators (wellbore breakouts, stress measurements, etc.) with earthquake focal plane mechanisms. Note that the mean and standard deviation of both sets of data are essentially identical.

determinations include the Bowman earthquake, which occurred in central S. Carolina and for which the stresses are inferred from surface wave modeling and first motion data, and a magnitude 4.1 earthquake that occurred at Clark Hill Reservoir just upriver from the SRS [Herrmann, 1986]. The maximum compressive stress direction at Charleston, SC is determined from the average of a series of single and composite focal mechanisms [Talwani, 1982], and is consistent with the development of wellbore breakouts during hydraulic fracturing at a well at Clubhouse Crossroads. Hydraulic fracturing measurements within the ADCOH site survey wells [Coyle et al., 1986; Moos et al., in press] indicate NE-SW compressive stresses at shallow depth near Westminster, SC. Composite focal mechanisms and wellbore breakouts within the uppermost 1 km at the Monticello Reservoir [Talwani et al., 1980; Zoback, et al., 1985] all indicate high compressive horizontal stresses and a NE-SW maximum compressive stress direction in north central S. Carolina. Shallow seismicity in the region, particularly within crystalline terranes, is predominantly reverse in character [Talwani et al., 1980]. These results present a consistent picture of the stress orientations near the SRS, in which the maximum horizontal stress (S_{Hmax}) is oriented roughly NE-SW, consistent with the broad, uniform, regional state of stress expected from a ridge push source.

There is little seismicity within the Savannah River Site and its immediate surroundings. Those earthquakes which do occur are quite small and are generally not widely felt. For example, the only earthquake for which a focal mechanism has been obtained is a very shallow (above 1 km), magnitude 2.6 earthquake which occurred at the SRS on June 9, 1985 [Talwani et al., 1986]. The earthquake appears to have occurred on the NW edge of the Dunbarton Basin near its intersection with a linear northwest-trending aeromagnetic anomaly. The location of the earthquake was postulated to have been controlled by the intersection of these two planes of weakness. One of the nodal planes corresponds roughly with the orientation of the Pen Branch Fault, and thus the earthquake was hypothesized to have occurred as a result of left-lateral strike-slip motion along this feature.

Previous Stress Measurements at the Savannah River Site

Hydraulic.fracturing and borehole televiewer data were obtained during the summer of 1988 in a series of shallow (less than 2000 ft deep) boreholes penetrating both crystalline basement outside of and Triassic redbeds within the Dunbarton Basin (see Fig. 1). The results present a picture of the in situ stresses at relatively modest depth beneath the SRS which is consistent with regional stress indicators (see Fig. 3).

Figure 4 presents stress magnitude determinations within SSW-1, SSW-2, and DRB-8 [after Zoback et al., 1989a]. Stress magnitudes are quite high, consistent with other results within the region and with those for exposed crystalline terranes elsewhere.

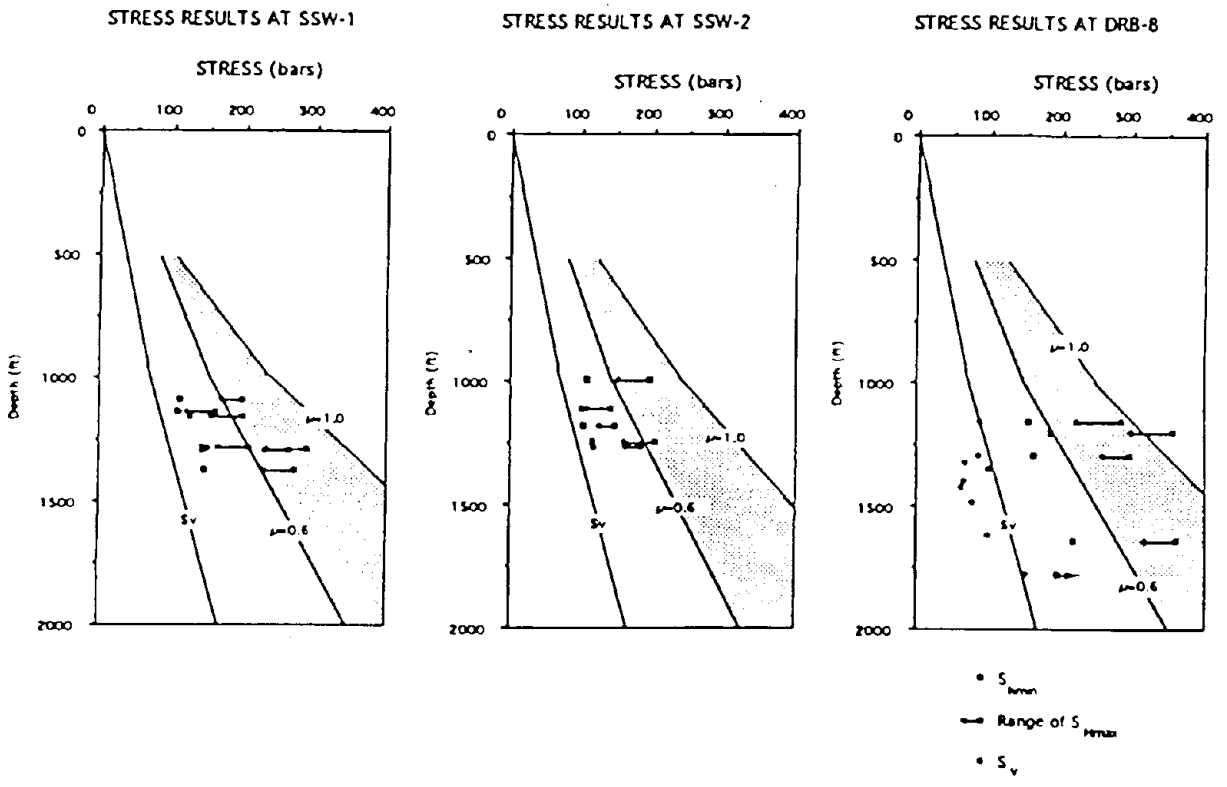

Figure 4 Stresses as a function of depth measured by hydraulic fracturing in SSW-1, SSW-2, and DRB-8 [after Zoback et al., 1989a]. Also shown in each case are the vertical stress (calculated by assuming a density in sediments of 1.9 gm/cm^3 and in basement of 2.8 gm/cm^3) and the limits on horizontal stresses for reverse faulting imposed by frictional constraints. Note that although stresses measured in DRB-8 are larger than in the other wells, all three show quite high horizontal stresses in the uppermost 2000 feet beneath the SRS.

Figure 5 presents the orientations of hydraulic fractures induced during the tests within SSW-1, SSW-2 and DRB-8. These were obtained both using oriented impression packers and by analysis of borehole televiewer logs run after the hydraulic fracturing tests were completed. They indicate a consistent, approximately N65°E orientation of maximum horizontal principal stress within the uppermost basement interval outside of the Dunbarton Basin.

Figure 6 presents a histogram of the orientation of maximum principal stress inferred from the azimuths of wellbore breakouts detected using a borehole televiewer within DRB-11. These occurred within Triassic redbeds over an interval from 1225 to 1325 feet below ground level, within the depth range in which televiewer logs were obtained in the other holes drilled outside the basin. Their orientation suggests a N55-70°E

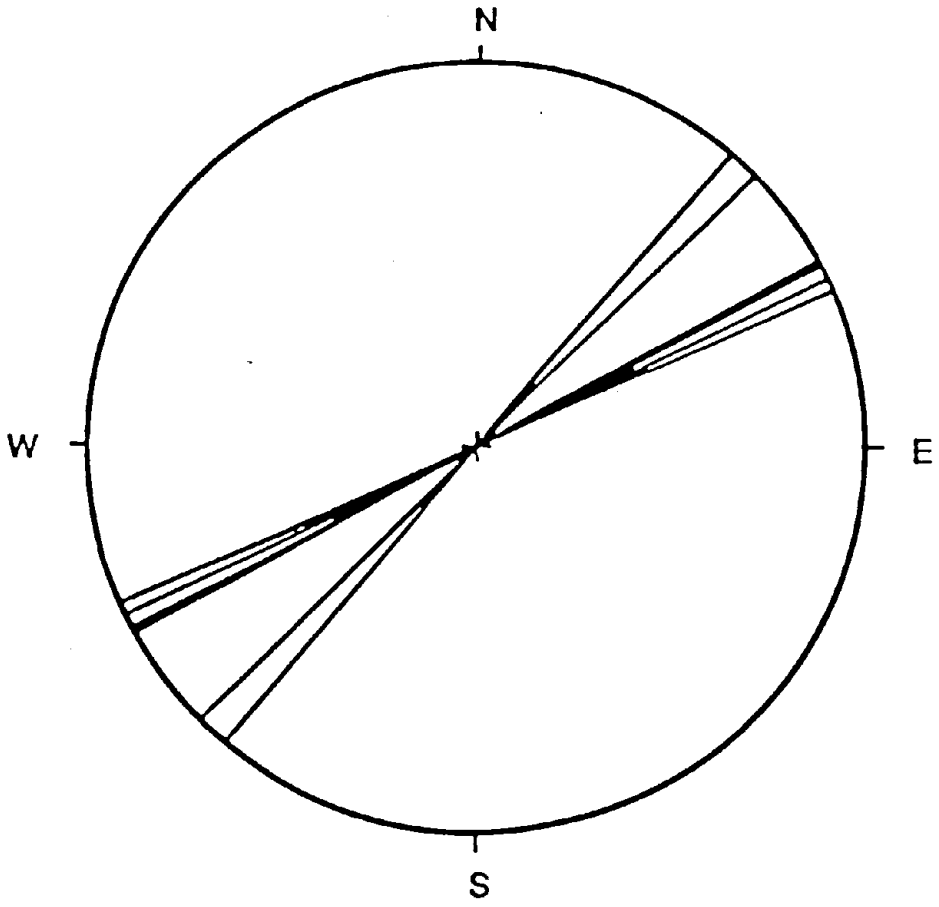

Figure 5 Orientations of a subset of six hydraulic fractures for which these could be obtained using impression packers and a borehole televiewer in Holes DRB-8, SSW-1 and SSW-2. These indicate a NE-SW direction of maximum compression.

orientation of maximum horizontal stress, similar to that inferred from the orientations of the hydrofracs shown in Fig. 5. The fact that breakouts were detected only within this well implies that stresses at these shallow depths are large enough to generate breakouts within the redbeds, but too low to cause wellbore failure within the crystalline rocks outside the basin. However, it is unclear whether this is a consequence of the greater strength of the crystalline rocks, or whether stresses outside the basin are somewhat lower than those inside the basin. As discussed below, breakouts were detected during this study within the crystalline rocks penetrated by the NPR hole, but only at depths greater than those for which data was available in the earlier holes.

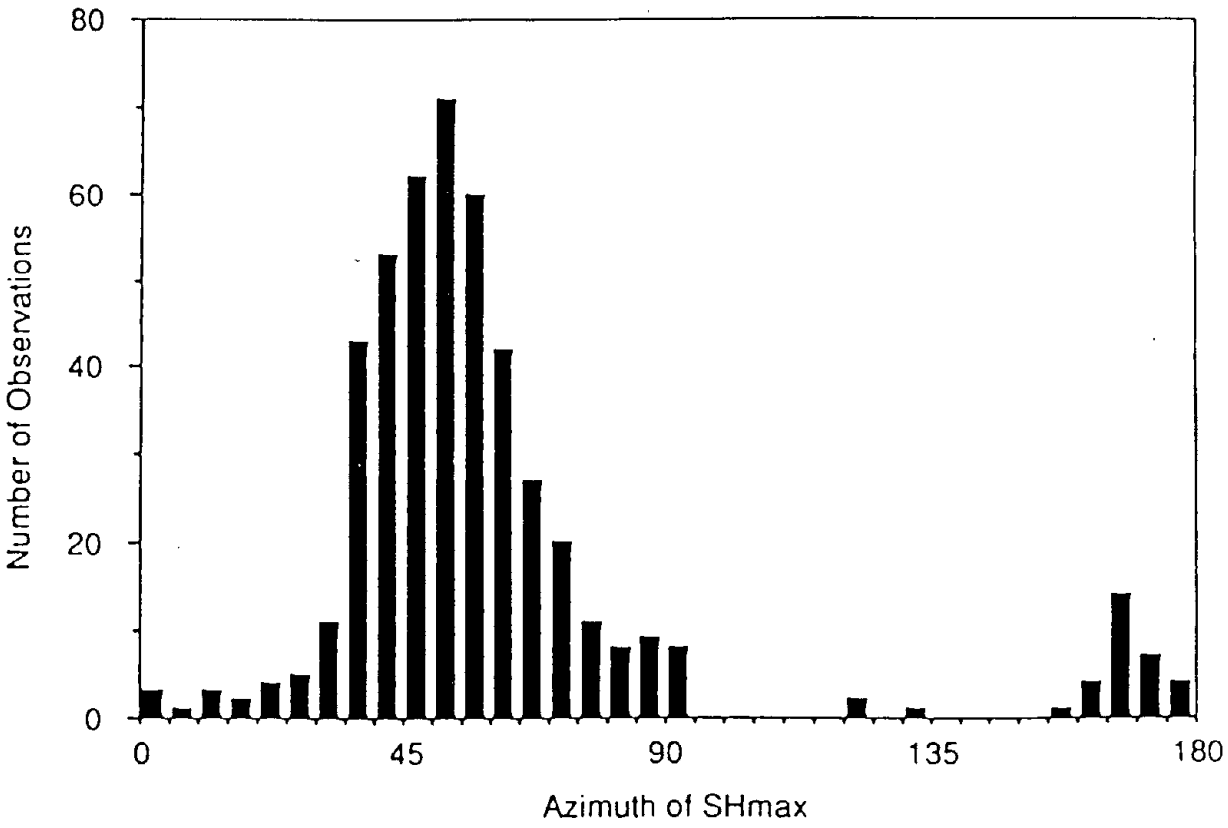

Figure 6. Histogram of maximum compressive stress orientations inferred from breakouts detected with the borehole televiewer within Triassic redbeds penetrated by Hole DRB-11.

Although the results shown in Fig. 4 imply high (reverse-faulting) horizontal stresses at shallow depths, it is unclear whether this stress state can be extrapolated to greater depths. For example, in the deep mines of South Africa where a reverse faulting stress regime is observed to a depth slightly less than 1 km, a normal faulting stress field is observed at greater depth [Brace and Kohlstedt, 1980]. A very similar case (reverse faulting at shallow depth and normal faulting at greater depth) has been documented at Oroville, CA [Anderson and Zoback, 1988]. Furthermore, stress measurements in Fennoscandia [Stephannson and Angman, 1986] on the Canadian shield [Brace and Kohlstedt, 1980] and near Monticello Reservoir in South Carolina [Zoback and Hickman, 1982] all show very high horizontal stresses in the upper ~1 km that apparently do not extend to greater depths. It is primarily for this reason that measurements were initiated in the NPR Hole, where a continuation of previous in situ stress determinations to almost 4000 feet was expected to be sufficient to answer the question of whether the shallow reverse-faulting stress regime beneath the SRS extends to greater depths.

Stress Measurement Program in the NPR Hole

The NPR hole was drilled to a depth of approximately 4000 feet near the center of the Savannah River Site (Figure 1). The measurements we conducted included a complete borehole televiewer log of the hole, and a total of twelve attempted hydraulic fracturing tests. Other measurements available for this hole included a magnetically oriented borehole deviation survey, a suite of geophysical logs, and a series of cores taken intermittently during drilling. Selected hydraulic fracturing test intervals were reoccupied with an impression packer to capture the precise orientation of the hydraulic fractures, and a repeat televiewer log was conducted at the conclusion of the impression and hydraulic fracturing tests to attempt to image the induced fractures acoustically. With the exceptions noted below, these measurements were conducted within the strict guidelines of a Level QA-1 quality assurance program developed expressly for this work [SAIC, 1991]. Appendix N summarizes the drilling and measurement timetable, and details of each stage of the work are presented briefly in this section, before proceeding to an analysis of the results.

Hole Description

The NPR Hole was drilled as part of a seismic attenuation study undertaken by the US Geological Survey to allow the emplacement of a geophone within the uppermost basement beneath surface sediments at the Savannah River Site (Fig. 1). As such, the well

was continuously cored to 1153 feet, at which point the hole penetrated a few tens of feet into basement. Saprolite was encountered at 1058 feet, and fine to medium grained granitic gneiss was recovered from about 1064 feet to 1153 feet. At that point the well was cased to 1046 feet, using 8" i.d. casing. A reversed seismic profile was then conducted with a wellbore clamped geophone emplaced near total depth. After a period of several months, during which the geophone was left in the hole to record local seismic activity, it was removed and the well was deepened to its final depth of 4000 feet. This phase of drilling was initiated using a percussive air-hammer and a 6 1/8" bit, which allowed rapid penetration. Air drilling was halted at a depth of 2177 feet due to extremely rapid influx of water. After cutting a core to 2187 feet, a decision was made to switch to standard rotary drilling, using a 5 7/8" bit. Drilling continued until approximately 2200-2205 feet, when the drillers encountered lost circulation problems. The hole was cemented back to 1978 feet, and drilling continued. The interval 2500-2530 was characterized by relatively soft rock (drilling was quite rapid), but otherwise drilling continued without encountering anomalous materials to total depth.

Short sections of core were recovered at intervals of approximately 500 feet. The core reflects typical basement geology, varying from a hornblende-biotite gneiss to a feldspar biotite gneiss. We selected three sections of core for sampling for laboratory strength testing by SAIC. These include (1) 1957-1958', a slightly altered hornblende-rich gneiss, (2) 3402-3403' - a sample which contains an intermediate amount of hornblende, and (3) 2993-2994' - a low hornblende, quartz / 2 feldspar biotite gneiss.

Geophysical Logging

Geophysical logs were recorded by the US Geological Survey after drilling was completed at a depth of 4000 feet. These included caliper, natural gamma, gamma-gamma density, neutron porosity, acoustic-wave (compressional) velocity and first-arrival amplitude, temperature, and formation and fluid resistivity. The data, in digital form, were transferred to disks and copied for presentation in this report. Although developed for sedimentary environments, these geophysical logs are also useful to characterize physical properties variations within crystalline rock [see, for example, Paillet, 1991].

Figure 7 presents the log data (with the exception of temperature and fluid resistivity) plotted as a function of depth in the hole. The caliper log shows quite clearly an abrupt decrease in hole size below 1076 feet, where deepening of the hole after emplacement of casing began. Although the diameters measured by the caliper appear to be a somewhat large compared to the reported drill-bit sizes used, there is also a small hole

size decrease evident at approximately 2170 feet, coincident with the commencement of rotary drilling and the consequent bit size decrease. Also, the hole appears to systematically decrease in diameter with increasing depth. Natural gamma emissions seem to have a roughly bimodal distribution; unusually high values indicate a more felsic rock (e.g. the 2-feldspar biotite gneiss, a sample of which was cored at 2993 feet), whereas

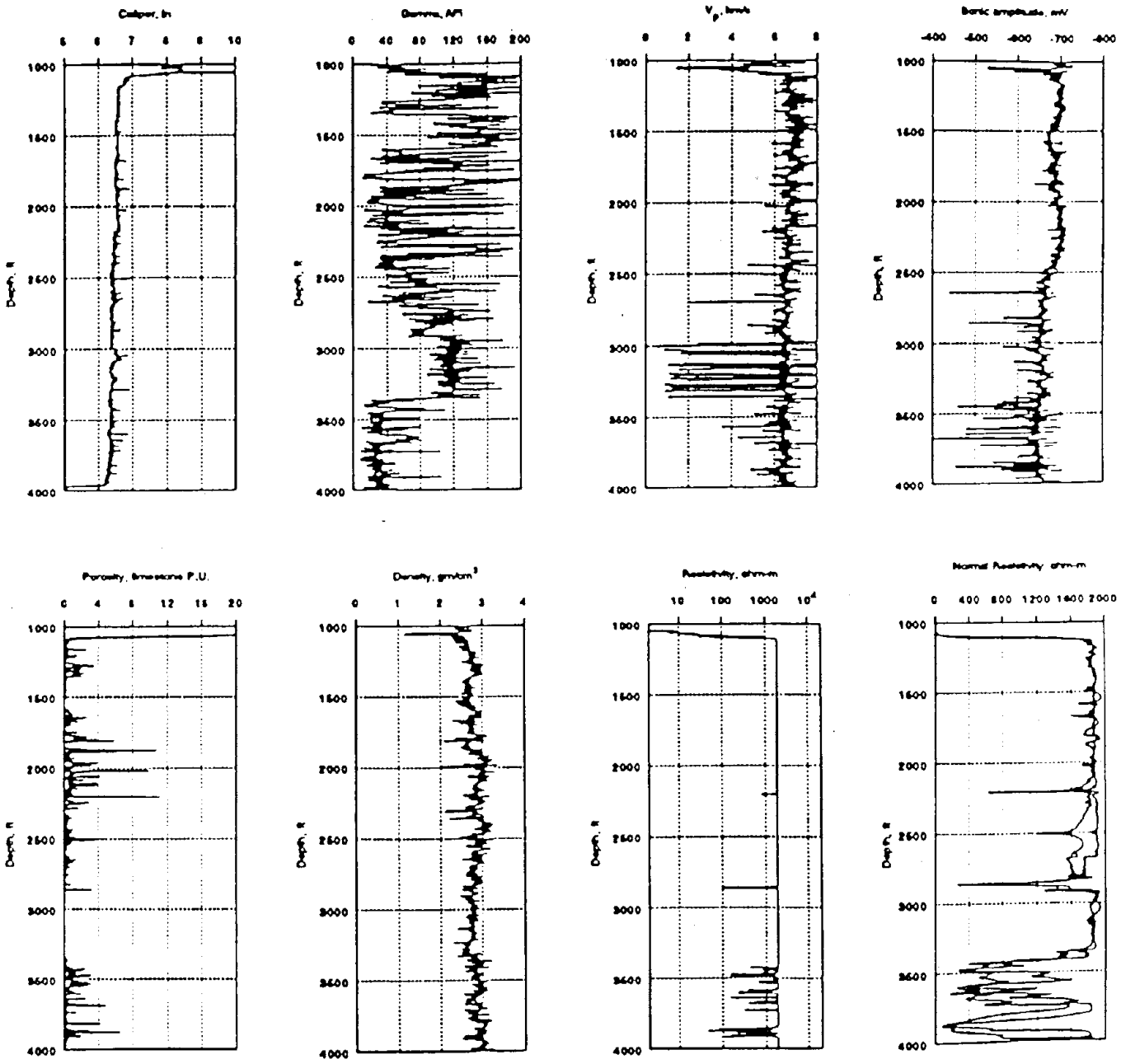

Figure 7 Geophysical logs recorded by the US Geological Survey (courtesy of Jerry Idler, U.S.G.S. Doreville, GA) in the NPR Hole.

much lower natural radiation is measured in the more hornblende-rich gneiss, samples of which were cored at 1957 and 3400 feet depths. Densities measured by logging are high (averaging more than 2.8 gm/cm^3); more felsic rocks have somewhat lower densities, whereas densities in more mafic intervals approach, and, in some cases exceed, 3.0 gm/cm^3. Higher apparent porosity and lower resistivities measured in less felsic rocks, particularly below about 3350 feet, may be due to the presence of hydrogen in alteration products, as the one core recovered from 3400 feet was somewhat altered. In the deepest section of hornblende rich gneiss, where electrically conductive intervals coincide with apparent porosity increases, these may also be zones of higher porosity (possibly related to fracturing). Pronounced low resistivity intervals are found at 2170 feet, corresponding to the zone of rapid water influx, and at 2500 feet (a zone of "softer" rock during drilling). Low resistivities were also measured over the interval 2850-2880 feet, where a number of sub-horizontal fractures, including a pronounced enlarged zone at 2863 feet, intersect the well (see also the BHTV data, Appendix L). Sonic amplitudes are lower in these same intervals, an effect which is consistent with the presence of fractures. Amplitudes are also lower and more variable in the deepest section of the well. However, acoustic velocities are quite high throughout (6.5 km/s to as much as 7 km/s).

These log responses characterize the rock as a very low porosity, high intrinsic velocity, high density material, reveal characteristic differences between mafic and more felsic materials, and appear to support observations in other areas that fracturing is quite significant in controlling the properties in situ of crystalline rock. For the purposes of this report, we can extract two useful pieces of information from these results. First, by integrating the density log we can calculate a fairly reliable estimate of the value of the vertical stress, S_v. Second, the apparently extremely low porosities and lack of pore connectivity implied by the very high resistivity allows us to use an hydraulic fracturing breakdown equation which ignores the in situ porosity, and uses the total stresses rather than the effective stresses to determine the value of S_{Hmax} [see, for example, Schmitt and Zoback, 1991].

Hole Deviation

As proper interpretation of the hydraulic fracturing results requires that the borehole be drilled within approximately 6° of vertical [SAIC, 1991], a wellbore deviation survey was carried out by Eastman Christensen Company on 3 March 1992. The results, presented in Appendix G, indicate that the wellbore meets the general requirements of the QA document above a depth of 3850 feet.

Borehole Televiewer Logging

The borehole televiewer (BHTV) is a device that acoustically scans the borehole wall to produce a magnetically oriented image of wellbore surface roughness and shape. It is described in detail by Zemanek et al. [1970], and its operation and the analysis of the resulting data are specified in the QA procedures prepared for this task [SAIC, 1991].

A BHTV log was run in the NPR hole prior to the hydraulic fracturing tests to (1) identify sections of the hole without pre-existing fractures or enlargements that are most favorable for hydraulic fracturing, (2) detect and characterize wellbore breakouts (see below), and (3) detect and characterize natural fractures and foliation. More than 14 intervals were picked from the televiewer data as candidates for hydraulic fracturing tests. Almost all of these were in the interval above 3500 feet, as the borehole wall was extremely rough in deeper sections of the hole (within the lowermost mafic section), making it more difficult for packers to seal properly, and fewer fracture-free intervals were available. A borehole televiewer survey was also run after hydraulic fracturing (and after use of a soft-rubber impression packer) to help determine the orientation of the induced fractures.

After digitization and preliminary processing following procedures outlined in Barton et al. [1990], the data were azimuth shifted to correct for magnetic declination and magnetometer offset, and the resulting data are presented in Appendix L. Calibrations of magnetic orientations and of the conversion factors between the acoustic time-of-flight of the pulse and wellbore radius were carried out both before and after logging, and are reproduced in Appendix K. Field and digitization QA forms are presented in Appendix J.

A summary of the logged depths (referenced to ground level) both for the pre-fracturing and post-fracturing BHTV logs is presented in Table I. Included in this Table are depth checks made during each logging run of the water level in the hole, the bottom of casing, and the depth recorded when the transducer was re-positioned at ground level at the end of the log. These depths are typically repeatable to within approximately one foot (except water level, which is often deeper after the log). In general we reference all depths

to our wireline, as depths of the hydraulic fracturing test intervals are chosen from the televiewer data and verified using the wireline during the test sequence. This is particularly valuable for the results presented here, as in this experiment a systematic pipe tally error was not detected until midway through the test sequence (see below and Appendices).

Table I: Borehole televiewer depth checks, in feet

Run	Water level in/out	Casing in/out	Re-zero
Pre-frac	100/104	1049/1048.8	-0.5
Post-frac	103/105	1048/1048.5	0

Hydraulic Fracturing

The hydraulic fracturing technique is a stress measurement method that relies on the fact that, once a borehole is drilled, the far-field stresses are concentrated in a known way in the region around the wellbore [Hubbert and Willis, 1957]. A typical test proceeds as follows: After isolating a short vertical section of the hole which contains no pre-existing weaknesses or fractures, the fluid pressure in the interval is increased rapidly until a new fracture is created. Flow into the interval is stopped almost immediately after the fracture is created, and the pressure decay of the closed system is monitored. After a stable pressure is achieved the system is drained, and the process is repeated a number of times to re-open the newly created fracture. Fluid pressure and flow rates into and out of the test interval are continuously monitored throughout the test, and analysis of the resulting pressure and flow rates vs. time allows determination of the magnitudes of the in situ stresses around the wellbore at the test depth. The precise methodology and analysis techniques have been extensively reported [see Haimson and Fairhurst, 1967; Hickman and Zoback, 1983; Baumgärtner and Zoback, 1989; Hayashi and Sakurai, 1989], and the methods employed here generally follow those outlined therein [see also SAIC, 1991].

Hydraulic fracturing tests were attempted twelve times within the NPR hole (see Table II). All pressure and flow rate data were recorded at the surface in both analog and digital form. The surface pressure transducers were calibrated against a 343 bar (5,000 psi) full scale Heise gage, which itself was calibrated prior to and following the field tests (see Appendix E for Heise calibrations and Appendix I for the surface transducer calibrations). We also recorded the first four tests on a pair of downhole pressure recorders positioned immediately above the packers. However, we use the surface pressures for these analyses, as the only difference observed between these and those recorded downhole is the static pressure head, which can be calculated using an hydraulic

head gradient of 0.45 psi/ft, corresponding to a density of 1.0 gm/cm^3 for the hydraulic fracturing fluid (see Appendix I). The surface-recorded data are plotted as a function of time in Appendix I, along with brief discussions of the characteristics of each test and the results of the analyses of the pressure-time histories. Also included (in Appendix H) are annotated analog chart recordings of the pressure and flow rate data. After completion of the first eleven hydraulic fracturing attempts, two impression packer runs were made to provide information on the orientations of the fractures generated during each test. Due to curtailment of the amount of time available to conduct the field tests, not all of the test depths were impressed (see Table II), and only one fully oriented impression test was run, for the test at 2406.1 ft. Although a BHTV survey was run after completion of the impression packer runs, not all of the fractures could be identified unambiguously from these post-frac surveys. This is not in accordance with generally accepted procedures, and the results of the analyses, particularly the magnitude of the maximum horizontal stress (S_{Hmax}), must be considered in light of this fact.

Table II: Summary of hydraulic fracturing measurements

Test[1]	Tally depth	Wireline depth	Result	Impressed	Post-frac BHTV
1	1242	≤ 1240.2	good frac	Y	Y
2	1540	1535.4	horizontal		Y
3	1853	1838.8	horizontal		Y
4	1940	1936.6	good frac		
5	2411	2406.1	inclined frac	Oriented	Y
6	3658	3649.4	pre-existing frac		Y
7	3410	3401.7	good frac	Y	Y
8	3420	3410.6	good frac	Y	Y
9	3349.2	3339.6	leak		
10	3340	3328.3	leak		
11	3188.5	3179.3	leak		
12	2100	2091	good frac		

[1] In chronological order

Results

Stress Magnitudes

Table III presents the stress magnitudes calculated from pressures measured during the hydraulic fracturing tests. All pressure values refer to downhole pressures in bars, calculated by adding to the measured surface pressure the weight of the water column from the interval to the surface, using an hydraulic head gradient of 0.45 psi/ft (see Appendix I). These include the breakdown pressure, P_b the instantaneous shut-in pressure, ISIP, the crack tip closure pressure (CTCP, Hayashi and Sakurai [1989]), and the fracture re-opening pressure, $P_b(T=0)$ that were determined from the pressure data recorded during the tests. Shut-in and breakdown pressures were determined in a number of different ways, to reduce uncertainties in their determinations. CTCP was determined from plots of dt/dP vs. P following the methods outlined in Hayashi and Sakurai [1989]. ISIP was determined from (1) the "knee" in the slope of the pressure-time curve after pumping stops [Hickman and Zoback, 1983] and (2) plots of dP/dt and P vs. t [Baumgartner and Zoback, 1989]. Breakdown (P_b) and fracture re-opening ($P_b(T=0)$) are computed by (1) picking the deviation from linearity of P vs. t during inflation, and comparing the shapes of these curves between cycles 1 and 2 [Hickman and Zoback, 1983] and (2) plotting the deviation from linearity of P vs. pumped volume [Baumgartner and Zoback, 1989]. In some cases these measurements were verified by looking at system compliance vs. pressure [e.g., Baumgartner and Zoback, 1989]. All of the pressure values determined using these techniques are presented in Appendix I; the values chosen for presentation in Table III and subsequent determination of the in situ stresses are noted in the Appendix. Examples of each of these methods applied to data from the NPR Hole are shown in Figure 8.

Determination of the stress normal to the surface of an hydraulic fracture is subject to a number of uncertainties. Those related to determination of ISIP are generally associated with system compliance and loss of fluid due to leaks and infiltration into the formation, and can be overcome by using a variety of methods, as we do here. However, it has recently been suggested that ISIP over estimates the stress normal to the fracture, and that a better estimate of this stress is the pressure at which the crack tip begins to close, CTCP [Hayashi and Sakurai, 1989]. We find, based on analysis of the data presented here, that although ISIP can be larger than CTCP, in agreement with Hayashi and Sakurai [1989], this relationship does not always hold (Appendix M). For example, ISIP is between the upper and lower bounds of CTCP for Frac 1; CTCP is essentially equal to ISIP for Test 8, and intermediate between ISIP computed using methods (1) and (2) for

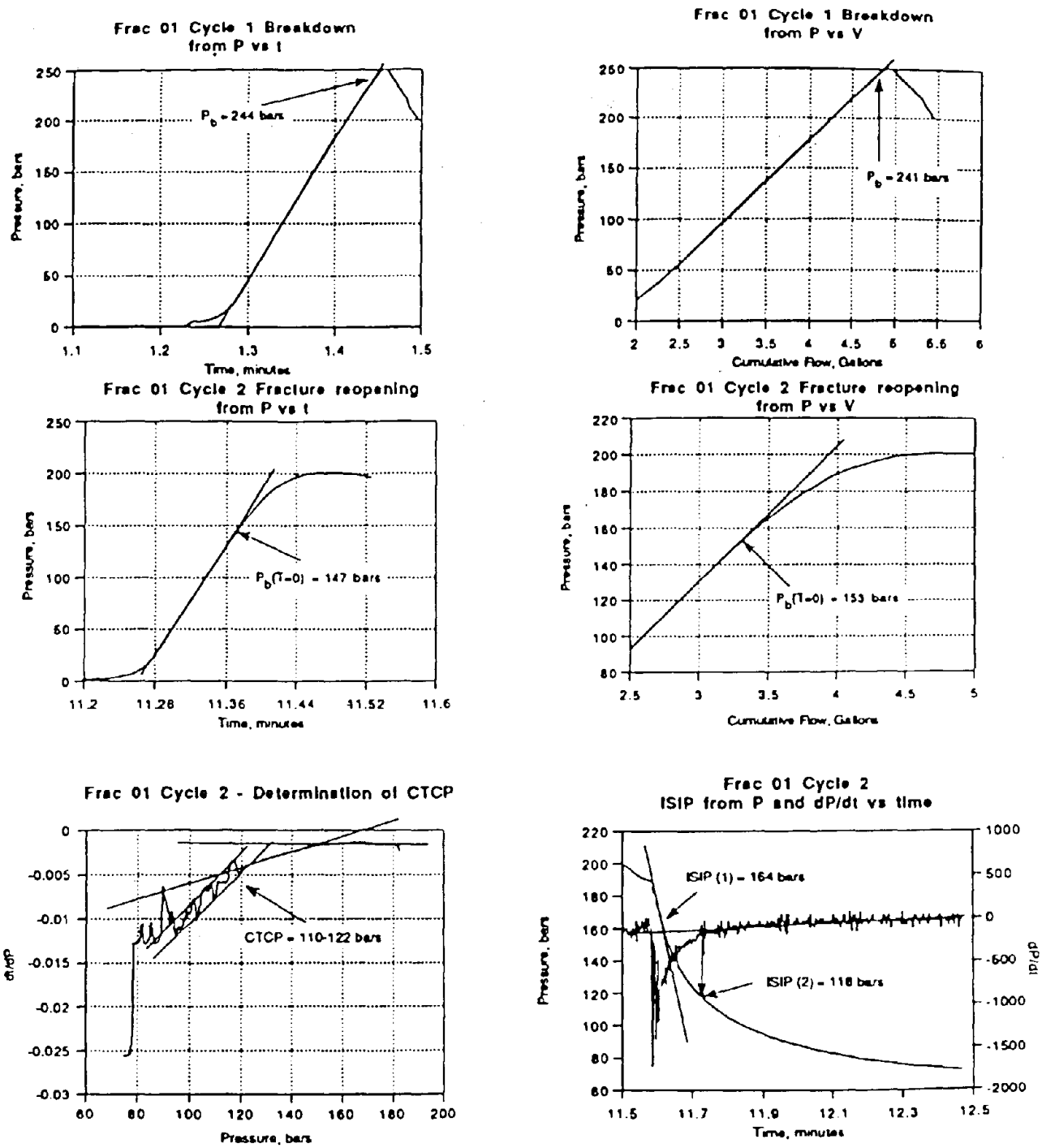

Figure 8 Example of the application of the various methods for determining P_b, $P_b(T=0)$, ISIP, and CTCP, as applied to data from Frac 1 at 1240.2 feet depth in the NPR Hole. Pressures are those measured at the surface.

Tests 7 and 12. In Test 5 CTCP is less than ISIP for Cycle 2, but greater for Cycle 4. In Test 4 Cycle 5 CTCP is again greater than ISIP determined using method (2). Therefore, we use CTCP and ISIP method (2) interchangeably to constrain the range of reasonable values for the stress normal to the fracture. Although this leaves open the question of which technique is more appropriate for stress determination, we feel that using both methods in this way is a more reasonable approach than one in which we choose, *a priori*, one or the other.

Unless otherwise noted, the least horizontal stress was determined in each case from ISIP and/or CTCP measurements taken during the second cycle of each hydraulic fracturing test. This is a reasonable approach both in cases where the least horizontal stress is less than and greater than the vertical stress, as in either case measurements made during the first cycle generally reflect near-wellbore effects, and where S_3 is vertical the fracture turns and later cycles measure S_v. In one test, however, we use Cycle 1 to determine S_{hmin}, as the fracture clearly rotated into the horizontal prior to the second cycle shut-in.

As there is also considerable discussion about the importance of pore pressure in fracture reopening, the maximum horizontal compressive stress was computed using the Hubbert and Willis (1957) formula as modified by Bredehoeft et al. (1976) both with and without pore pressure, to provide upper and lower bounds on S_{Hmax}:

$$3\,S_{hmin} - P_b(T=0) - P_p \le S_{Hmax} \le 3\,S_{hmin} - P_b(T=0), \qquad (1)$$

Tensile strength was computed from the difference between P_b and $P_b(T=0)$. Both P_b and $P_b(T=0)$ were determined from the deviation from linearity of plots of cumulative flow vs pressure for the first and the second cycles of each test, respectively, unless otherwise noted. This method was chosen, rather than using the pressure-time curves, because the results were more consistent using this technique. Where first and second cycle pressurization rates were identical the two methods yielded essentially the same results. The range of minimum stress values in Table III reflect the uncertainties in picking pressure values. The range of maximum stress values is much larger, as it also takes into account the effect of including and ignoring the pore pressure term in Eqn. (1). When using Eqn. 1 to compute S_{Hmax} we assume, even in the absence of verification, that fractures initiated as vertical cracks at the azimuth of S_{Hmax}.

Table III: Hydraulic fracturing stress magnitudes, bars

Depth	P_b (cycle 1)	P_b(T=0)	Tensile Strength	P_p[6]	S_{hmin} (ISIP/CTCP)	S_{Hmax} (w/o P_p)	S_{Hmax} (w/ P_p)	S_v (ISIP/CTCP)	S_v logging	Implied S_{Hmax} Orientation[4]
1240.2	279	191	88	35	148-160	253-289	218-254		78	N75°E, vert(?) (BHTV)
1535.4	353	93	260	45	-	-	-	87[5]	105	horizontal frac (BHTV)
1838.8	414	105	309	54	-	-	-	103[5]	132	horizontal frac (BHTV)
1936.6	365	290-310[3]	55-75	57	≤236-238	398-424	341-367		141	low tensile strength; no orientation
2091	353	150-156	197-203	62	188-190[1]	408-420	346-358	137-139[2]	157	No orientation rotated to horizontal
2406.1	327	206-222[3]	105-121	72	193-199	357-391	285-319	160-166[2]	187	Inclined, N58°E (I) rotated to horizontal
3401.7	339	218-230	109-121	102	196-206	358-400	255-297		278	probably vertical (I)
3410.6	355	255-265	75-100	103	235-239	440-462	337-359		279	probably vertical (I)

[1] from cycle 1 shut-in

[2] fracture rotated into horizontal, S_v from late cycle ISIP or CTCP

[3] from cycles 2 and 3

[4] BHTV - from televiewer data; I - from impression packer data (see below)

[5] from Cycle 2 ISIP

[6] Using 0.45 psi/ft and a water table at 104 feet depth

The magnitudes of the in situ stresses denoted in Table III are shown as a function of depth in the NPR hole in Figures 9a,b. Also shown is the expected magnitude of the vertical stress, S_v, computed by integrating the density logs recorded by the US Geological Survey and shown in Fig. 7. The pore pressure at depth was computed using the observed depth to the water table (104 feet) and assuming a water density of 1.0 gm/cm^3. A vertical stress magnitude of 58 bars was assumed for the top of basement, based on a sediment density of 1.9 gm/cm^3. These figures also include the results of previous stress measurements in Hole DRB-8 (re-analyzed using Eqn. 1).

Lines which constrain the magnitude of S_{Hmax} based on the frictional strength of well-oriented faults with coefficients of friction between 0.6 and 1.0 (within the range of laboratory measurements, see Byerlee, 1978]) are shown in Fig. 9a. These limits are computed from the assumption that a well-oriented fault will slip if the ratio of the effective maximum and minimum stresses exceeds its frictional strength:

$$(S_1 - P_p)/(S_3 - P_p) = ((1+\mu)^{1/2} + \mu)^2 \qquad (2)$$

It has been found that measured stresses in the crust generally fall within the range allowed by such a frictional strength criterion [e.g., Zoback and Healy, 1984]. Above about 2500 feet the constraint is imposed by the strength of reverse faults. For the tests at 3410 feet, where S_{hmin} is less than S_v, the faulting regime is strike-slip and the constraint on S_{Hmax} is computed using as S_3 the average value of S_{hmin} determined by hydraulic fracturing (see Table III). For convenience, we connect this point to the line defining the reverse faulting constraint at 2406 feet, where the hydrofrac-determined value of S_{hmin} is only slightly greater than the log-determined value of S_v.

Stress magnitudes measured in DRB-8 (open symbols) and NPR (solid symbols) are in excellent agreement. Furthermore, the intermediate depth range in the NPR hole where tests produced horizontal fractures overlaps a similar zone in DRB-8. It is not clear, however, whether this is due to lithologic control of fracture formation in both holes, to the variation in stress magnitudes with depth, or to a combination of both factors.

As shown in Fig. 9, horizontal stresses are quite high at shallow depth and close to the frictional limit for reverse faulting above 2500 feet. However, both horizontal stresses increase quite slowly with depth, and below a depth of about 2500 feet the least principal stress is horizontal. Taking the average value of S_{hmin} for the two measurements near 3400 feet, the magnitude of S_{Hmax} is only slightly less than that required to generate slip on well-oriented strike-slip faults.

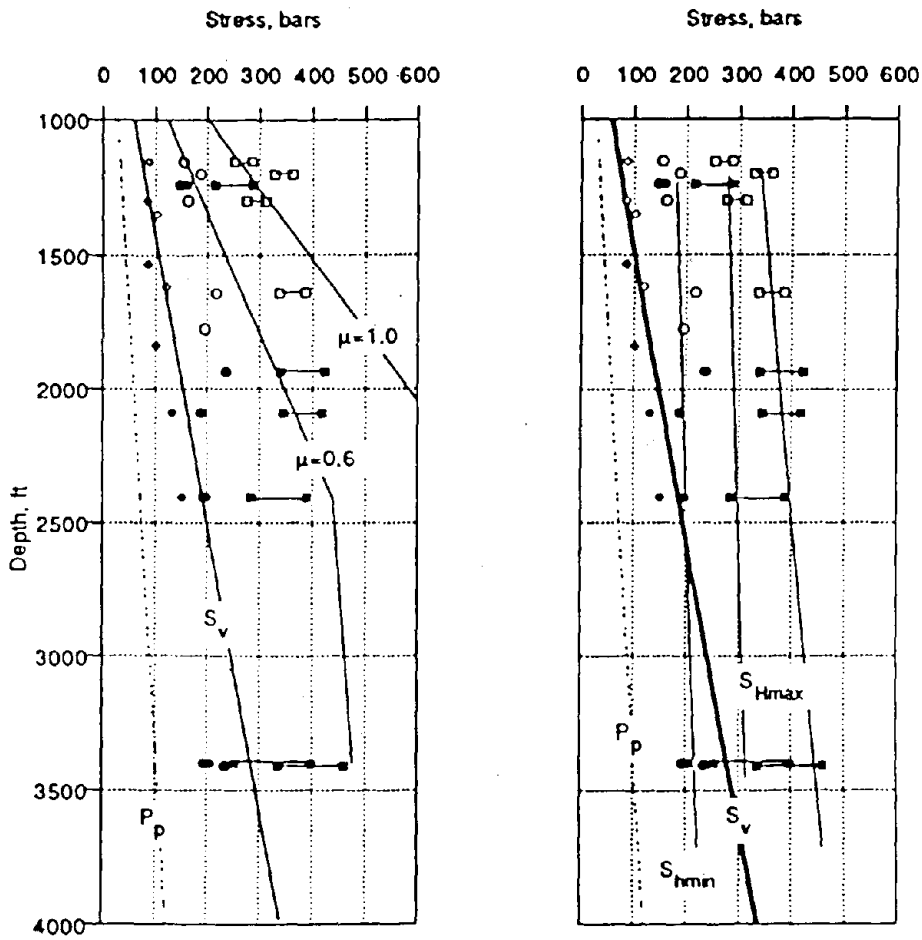

Figure 9 Stresses calculated from hydraulic fracturing tests conducted within the NPR Hole (solid symbols) and DRB-8 (open symbols). Squares are S_{Hmax}, circles are S_{hmin}, and diamonds are S_v. Also shown are the vertical stress calculated by integrating the density log shown in Figure 7, with an assumed value of 58 bars at the top of basement, based on a sediment density of about 1.9 gm/cm^3, and the pore pressure for a depth to water table of 104 feet, based on BHTV data. Lines showing the upper bound on the horizontal stresses for reverse faulting (above 2400 feet) and strike-slip faulting (below 2400 feet) with coefficients of sliding friction μ=0.6 and 1.0 are shown on the left. Shown on the right are best-fit lines to the calculated horizontal stresses. The upper and lower bounds on S_{Hmax} represent fits to the data ignoring and including, respectively, the pore pressure in Eqn. (1).

Averages to the best-fit lines through the upper and lower bounds of the hydrofrac-determined horizontal stresses have slopes of 0.015 bars/ft (including pore pressure) and 0.047 bars/ft (ignoring pore pressure) for S_{Hmax} and 0.021 bars/ft for S_{hmin}, compared to 0.095 bars/ft for S_v (Fig. 9b). While we impute no great significance to these slopes, it is important that the rate of increase of both horizontal stresses with depth is quite small. Based on our new data, the near-surface reverse faulting stress regime clearly does not persist to depths greater than about 2100 feet, similar to the cases of Monticello, South Africa, and the Canadian Shield mentioned above.

Stress Orientation from Wellbore Breakouts

Before proceeding to a discussion of the hydraulic fracture orientations, we present the results of analysis of wellbore breakouts imaged by the BHTV. Wellbore breakouts (see Figure 10) are defined as sections within which a wellbore is elongated due to compressive shear failure of the rock at the azimuth of S_{hmin} [e.g., Bell and Gough, 1983]. Zoback et al. [1985] presented a model for their formation in which the circumferential hoop stress exceeds the strength of the rock, causing compressive shear failure and subsequent enlargement of the borehole where the hoop stress is greatest (that is, at the azimuth of S_{hmin}). Moos and Zoback [1990] subsequently described a method whereby in situ stress magnitudes could be constrained by observations of breakouts in sections within which the rock strength is known and where failure does and does not occur. Therefore, in certain circumstances, both the azimuth and the relative magnitudes of the in situ horizontal stresses can be determined using observations of wellbore failure if the strength of the rock is known.

Breakouts were analyzed by examining cross-sections of the wellbore formed by superimposing four transducer scans. Thus each cross section represents a vertical distance of 1.3 inches, or 0.11 feet. Breakouts can be differentiated from wellbore enlargement due to drillbit or pipe wear by restricting the analysis to those sections within which the enlargements occur symmetrically on both sides of the hole, and have a rough-edged character. The entire data set was analyzed using these restrictive selection criteria, and a total of 680 individual breakout measurements was made.

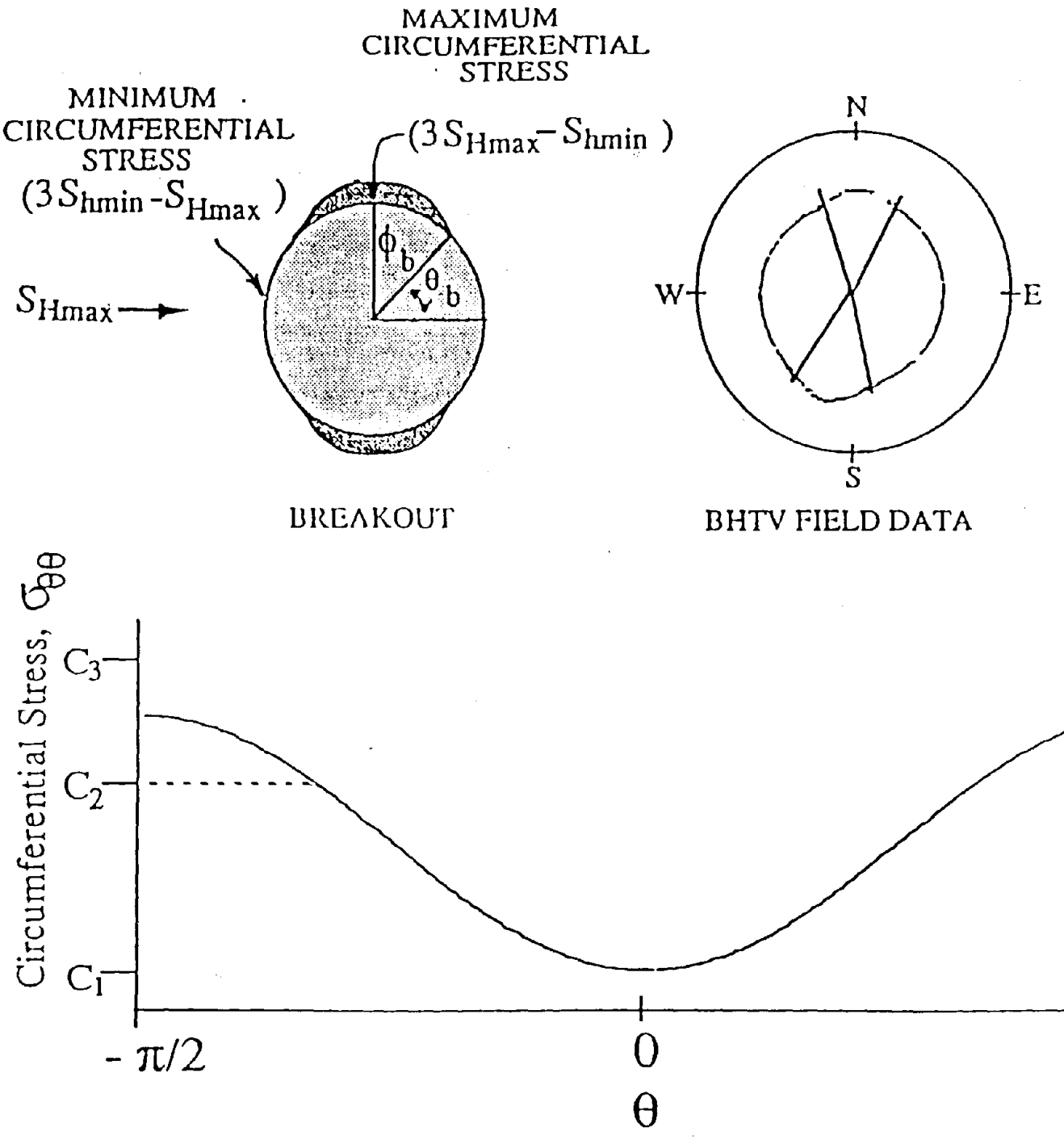

Figure 10 Schematic illustrating the variation of circumferential stress around a well drilled into the earth's crust (bottom) along with a diagram of the expected shape of a wellbore breakout (region of compressive shear failure) at the azimuth of the least far-field compressive stress (top left). Also shown is an example of a wellbore cross section from televiewer data in a breakout interval (top right).

A plot of the midpoints of the breakouts as a function of depth is shown in Figure 11. Breakouts begin in this hole at a depth of 1920 feet. However, they are intermittent above a depth of approximately 3000 feet. This is consistent with previous work, in which no breakouts were found within crystalline rock outside of the Dunbarton Basin to a total depth of more than 1820 feet (see above and Zoback, et al. [1989]). It is clear from this figure that the breakouts have a generally consistent NW-SE orientation. When examined

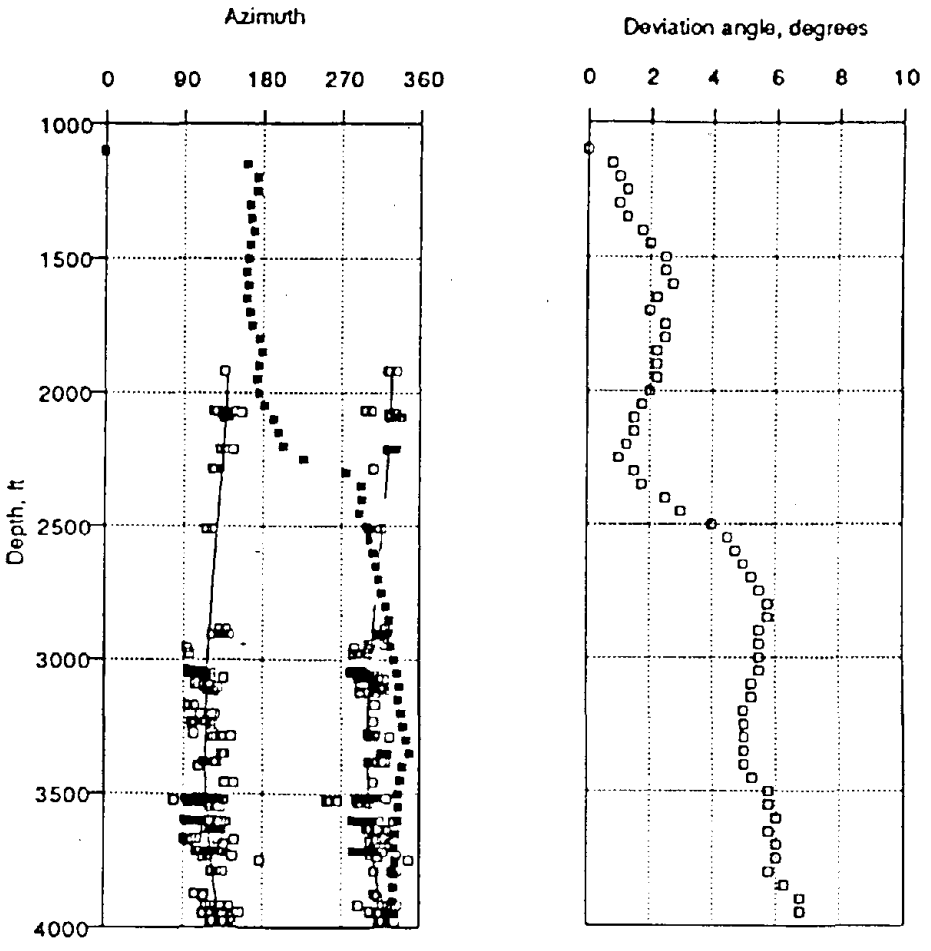

Figure 11 Breakouts and wellbore deviation within the NPR Hole. Breakout (open symbols) and deviation (solid symbols) azimuths are shown on the left; deviation angle on the right. Each point represents one breakout pick over a 1.3" interval of the wellbore. Deviations are plotted at the depths of the measurements, which were made every 50 feet in the hole. Also shown are 3rd-order polynomial fits to the breakout orientations.

in more detail, however, there is an apparent shift in the breakout orientations along the length of the hole. The breakouts at shallow depth (above 2500 feet) are rotated about 20 degrees clockwise, compared to deeper data. However, the deepest breakouts are beginning to rotate back towards the direction in which they form above 2500 feet, as can be seen in the data and as is emphasized by a 3rd-order polynomial fit to the breakout orientation data.

Also shown in Fig. 11 are the results of the deviation survey run by Eastman Christensen. It is interesting to note that at approximately the depth at which the breakouts become more common the hole deviation increases and turns in roughly the direction in which the breakouts form. This is not unexpected, as the rock is at failure during breakout formation, and it is easier for the bit to deviate towards the breakouts, where the rock is weakened by the failure process. Although when picking breakouts from dipmeter data it is generally necessary to eliminate intervals where the breakouts and hole deviation are in the same direction (to avoid contamination by pipe wear; see Plumb and Cox [1987]), the ability of the televiewer to produce a detailed cross-section of the wellbore allows us to easily distinguish between the two.

Figure 12 is a histogram of the direction of S_{Hmax} as determined from the breakout orientations detected along the length of the NPR hole. In this figure, the breakout picks in the NW quadrant are merged with those in the SE quadrant by subtracting 180° from their azimuths and then the resulting orientations are shifted 90°. As breakouts form in the azimuth of the far-field least horizontal stress, the mean of 33° ± 15° implies a maximum horizontal compression direction of N33°E for the region surrounding the NPR hole. This direction of maximum in situ horizontal stress is about 20-30° more northerly than suggested by results at shallower depth both in this hole (above) and in SSW-1, SSW-2, DRB-8 and DRB-11.

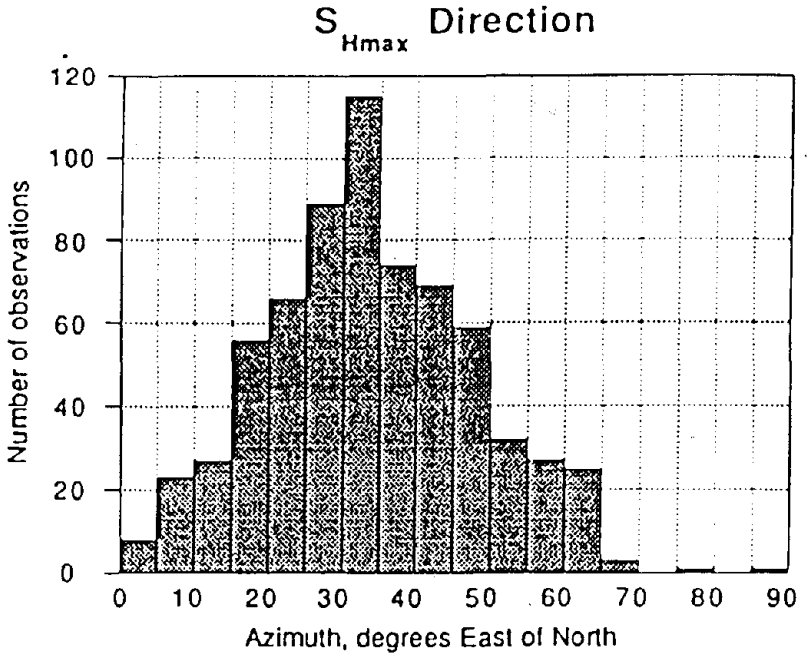

Figure 12 Histogram of S_{Hmax} directions inferred from the breakout data shown in Fig. 10. The average azimuth of maximum horizontal stress predicted from the breakout measurements is N33°E (±15°).

Hydraulic Fracture Orientations

The orientations of the fractures produced by hydraulic fracturing tests (see Table III) were determined in two ways. The first method employs a so-called "impression" packer [see Anderson and Stahl, 1967] to reproduce an image of the surface of the wellbore. The image is produced by pressing a packer (onto which a soft rubber sleeve has been attached) against the wellbore wall at a pressure above that required to reopen a previously created hydraulic fracture. By maintaining this pressure, a small amount of rubber is squeezed into the now open fracture, and when the packer is deflated a small ridge is left behind from which the trace of the fracture can be obtained. While the packer is inflated its orientation is determined through the use of a magnetic orientation device.

The first magnetically oriented impression was run to image the fracture produced at 2406.1 ft wireline depth. This impression image, with the center of the packer at 2404.9 feet, is reproduced in Figure 13, which shows the image of the 8.5-foot length of the impression packer. Only the lower half of the packer is shown, as no features were observed on the upper half. The orientation line is at a compass azimuth of N72°W, based

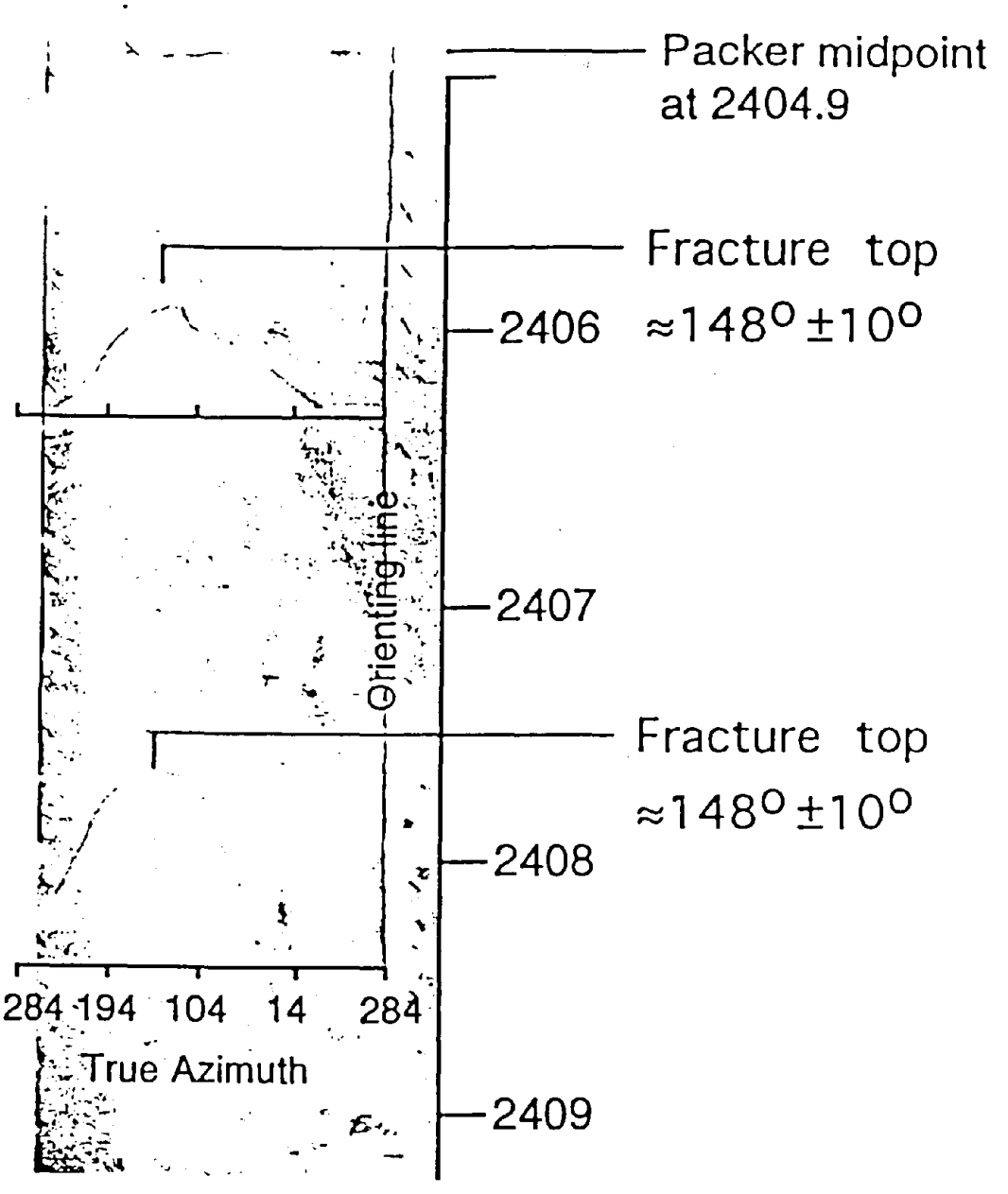

Figure 13 Tracing of the impression packer at a depth of 2406.1. This figure was made by scanning a color print of a photograph of the tracing made of the impression packer in the field. The faint lines on the images are the traces of fractures delineated by small raised markings on the impression packer. This packer was oriented using a magnetic device, and the known magnetic azimuth of a reference line of N72°W (azimuth 288°) was corrected for magnetic declination by subtracting 4 degrees.

on the Kuster single-shot key orientation of N40°W and a 32° counter-clockwise offset of the orienting line to the "key" (field notes, pp. 101; 104). With the image vertical, motion to the left is clockwise around the packer, or toward increasing azimuths (as illustrated in the scale). Two inclined fractures are apparent on this image, one at about 2406 feet, and a steeper fracture at 2408 feet. Based on the BHTV-derived wellbore radius of 2.9 inches and the known length of the packer of 8.5 feet, the shallower feature dips approximately 45°, and the deeper feature approximately 65°. The strikes are identical (N58°E); both were likely to have been within the 4-foot interval covered during the hydrofrac test. It is not clear from this image whether one or both of these features was opened during the test. However, their orientation is roughly consistent with the orientation of breakouts, indicating a NE-SW maximum horizontal stress direction. And, while these fractures are inclined, their dips (particularly for the steeper fracture) introduce a relatively small error in the computed magnitude of S_{Hmax} from the assumption that the fractures were vertical.

We also ran a single impression packer which was inflated at drill-pipe depths of 1242, 3410, and 3420 feet, to impress and image (without orientation) the fractures created by the hydrofrac tests at wireline depths of 1240.2, 3401.7, and 3410.6 feet. The purpose of this run was to verify the creation of vertical fractures during these tests, and to enhance the likelihood of seeing the fractures in BHTV logs run after the impression runs. The fractures recorded on the impression sleeve during this run are reproduced in Figure 14. A number of fractures are seen in this image. Most of these are nearly vertical, although sub-horizontal features about 1/4 and 3/4 of the way down, and one roughly 45° feature about 2/3 of the way down, are also seen. Two pairs of 180°-opposed, vertical fractures can be seen clearly extending approximately 3-4 feet along the lower half of the packer (identified as "Frac 1" and "Frac 2"). These are clearly the images of two separate, hydraulically-induced fractures. A third set, seen on the upper half of the packer, are separated by approximately 200°, and may indicate a third pair of hydraulically induced fractures (identified as "Frac 3?"). And, a number of other fractures dipping more than 70 degrees can also be seen. Based on this image, at least two and possibly all three of the tests which were impressed with this packer opened vertical fractures. In combination with the pressure records, which indicate a somewhat low tensile strength for the test at 1240.2 feet, it is likely that both of the deeper tests created vertical fractures ("Frac 1" and "Frac 2"). We attempted to verify this by investigating the pre- and post- hydraulic fracturing BHTV images of these and the other test intervals.

A BHTV log was conducted after the second impression run to record data over the intervals centered at wireline depths of 1240.2, 1535.4, 1838.8, 2406.1, 3401.7, 3410.6, and 3649 feet. Enhanced, grey-scale images of these post-frac logs are reproduced in

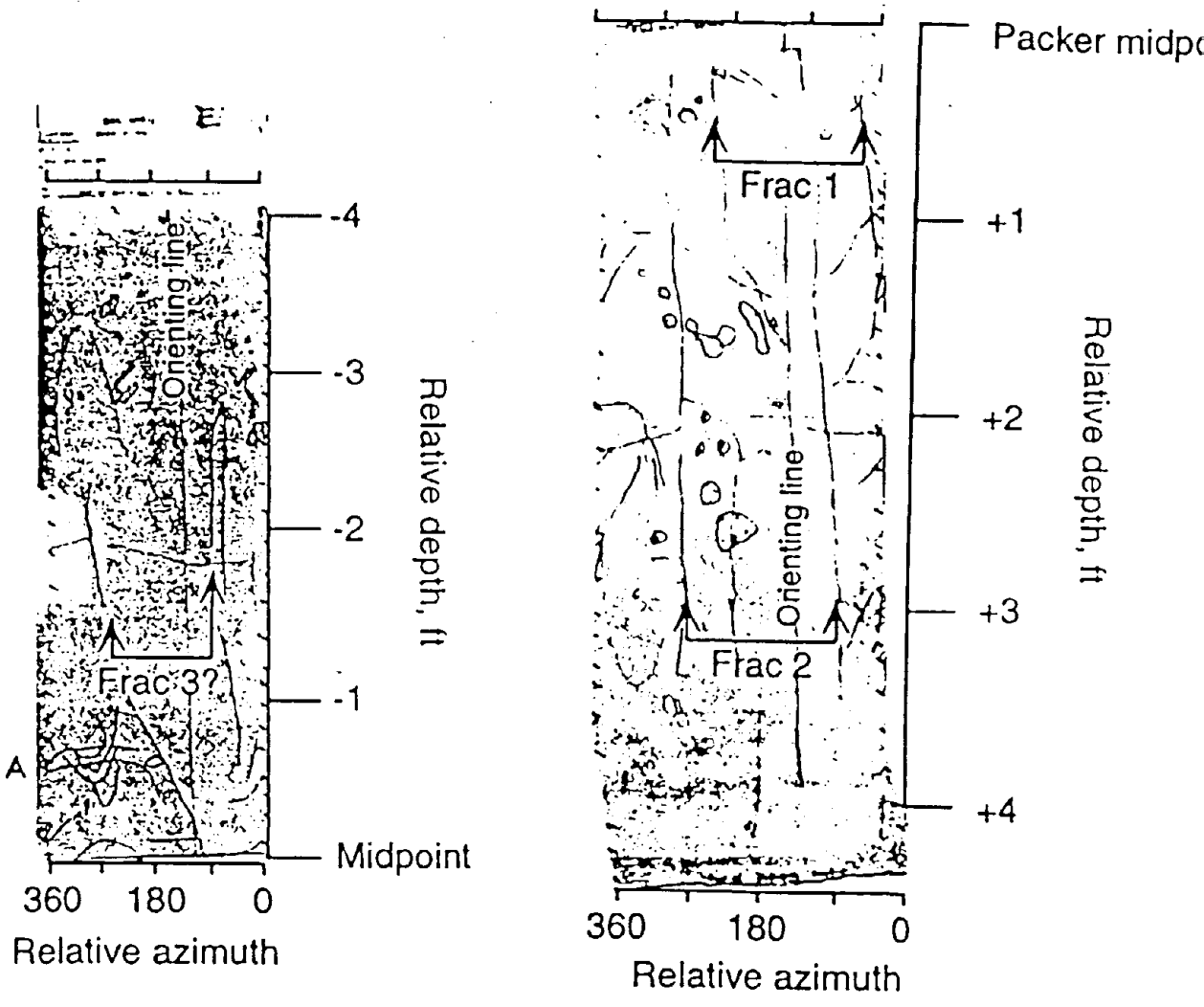

Figure 14 Tracing of the impression packer run at depths of 2042.2, 3401.7, and 3410.6. This figure was made by scanning a color print of a photograph of the tracing made of the impression packer in the field. The faint lines on the images are the traces of fractures delineated by small raised markings on the impression packer. As this packer was run at three depths and was not oriented, azimuths are relative. "Frac 1", "Frac 2", etc. are for identification purposes only and do not imply chronology.

Appendix M, along with pre-frac logs from the same intervals. These two logging runs can be directly compared, as the same gains and tool settings were used for both. And, although the fractures are generally more difficult to detect on these logs compared to the impression packers, several likely candidates can be seen in this data.

A small feature at 1239.5 feet is apparent at an azimuth of 255° in the post-frac data presented in Appendix M, from the interval centered at 1240.2 feet (see the arrow). This appears to be a short vertical fracture, which turns into the horizontal and disappears at about 1240 feet at an azimuth of about 270°. This is looks quite similar to feature "a" marked on the impression packer (Fig. 14), which has a short vertical section, below which it turns West into a series of sub-parallel horizontal fractures. And, the orientation of the vertical portion of the fracture of N75°E on the BHTV log suggests a similar orientation of S_{Hmax}.

A number of sub-horizontal fractures can be seen on the post-impression BHTV images of the intervals at 1535.4 and 1838.8 feet. In both cases, any one of these could have been opened to produce the pressure-time curves we observed during these tests.

Data from the interval in which the oriented impression was obtained (midpoint depth 2406.1) reveals the presence of a 65° west-dipping fracture at 2410.5 feet, equivalent to the steeply dipping fracture imaged by the impression packer at 2409 feet. There is no evidence in the BHTV data of the more shallowly dipping fracture immediately above this one.

The intervals at 3401.7 and 3410.6 are both characterized by considerable wellbore roughness. This makes it likely that small bits of rock embedded in the impression packer came from one of these intervals, but makes locating fractures on the BHTV images even more difficult. No vertical features can be seen in either interval to match those observed on the un-oriented impression packer.

Finally, inspection of the interval at 3649 feet explains why that particular test was unsuccessful - a series of shallow, east-dipping fractures intersect the wellbore within the test interval.

Discussion

The results presented above indicate that (1) horizontal stress magnitudes above 2100' are close to the limit constrained by the strength of well-oriented reverse faults, (2) the rate of increase with depth of the horizontal stresses is less than the rate of increase with depth of the vertical stress, and (3) the greatest horizontal stress drops below the values required to cause reverse faulting at a depth of approximately 2300 feet. This is similar to a number of other areas, as discussed above. In the depth range between 2400' and 3400' the difference between the maximum and minimum horizontal principal stress is nearly high enough to cause strike-slip faulting on well-oriented fault planes. This is illustrated in Fig. 15, which shows that over the entire range of depths studied in the NPR hole, the state of stress appears to be in equilibrium with the strength of well-oriented faults; above 2100' NW trending reverse faults appear to potentially active and between 2400 and 3400' N-S striking right-lateral and ENE striking left-lateral faults appear to be potentially active. The latter case appears to be consistent with the occurrence beneath the SRS of a shallow (<1 km depth) small magnitude (~M2.6) earthquake in 1985 (Talwani et al., 1986).

Of obvious importance is what this stress state means about the potential for damaging earthquakes to result from movement along the Pen Branch fault. Two issues are critical to this assessment - extrapolation of the measured stress magnitudes to greater depth and the orientation of the direction of maximum compression with respect to the strike and dip of the Pen Branch.

Considering first the issue of stress magnitudes, it is clear that if we attempt to linearly extrapolate the stress magnitudes we measure above 3400 feet to greater depth we encounter serious problems at depths of only a few km. First, the extrapolated maximum horizontal stress drops below the vertical stress, which implies an extensional state of stress in the midcrust within a region that is generally characterized by horizontal compression [e.g., Zoback and Zoback, 1991]. Second, because the gradient of the least horizontal stress with depth is so small, it drops below the hydrostatic pore pressure, which is physically impossible. Thus, linear extrapolation of the relatively shallow stress magnitudes in NPR to mid-crustal depth is not reasonable. This is not unusual as there is a substantial body of previous work indicates that stresses do not increase smoothly with depth. For example, in one well near the San Andreas Fault, stresses clearly increase in a step-wise manner between intervals within which the magnitudes are relatively constant [Zoback, et al., 1980]. We can observe a similar effect in the data from within the NPR and DRB-8 holes. Although we can fit lines through the stress data, as in Fig. 9b, it is equally reasonable to suppose that stresses increase in a step-wise manner (with one such step at about 1500 feet). What we can say with confidence is that the reverse faulting stress

regime observed at very shallow depth would promote reverse movement on NW striking planes, not NE striking planes like the Pen Branch. The tendency for strike-slip faulting observed at depths of 2400-3400' (which appear to be consistent with the occurrence of the extremely shallow 1985 earthquake) may also quite depth limited as the state of stress consistent with this event cannot be extrapolated to depth.

The precise orientation of the maximum horizontal stress at SRS is somewhat problematic. Figure 16 summarizes the stress orientations at each hole obtained both in this study and in previous work at the Savannah River Site [Zoback et al., 1989a]. The maximum horizontal stress is oriented in a generally NE-SW direction, sub- parallel to the ~N55°E striking Pen Branch Fault. The orientation of maximum stress in the deeper part of the NPR hole of N33°E indicates a distinctly more northerly direction of S_{Hmax} than shallower measurements (N66°E based on 1 vertical fracture orientation within DRB-8, about N63°E based on 2 excellent fracture orientations within SSW-1, N66°E based on one fracture orientation within SSW-2, and N55-70°E based on breakouts in DRB-11 within the Triassic Dunbarton Basin). The orientations of the two hydraulic fractures we measured within the NPR hole are ~N75°E at ~1240 feet, and ~N58°E at ~2400 feet, consistent with the previous work at similar depths. All of these measurements apparently indicate a counter-clockwise rotation of stress between the shallower (above 2500 feet) and deeper (2900-3800 feet) measurements. As the northeasterly segment of the Pen Branch fault strikes approximately N55°E (Fig. 1), a N33°E direction of S_{Hmax} might indicate the possibility for left-lateral strike-slip fault motion to occur if 1) both this stress orientation and that of the fault persist to greater depth and 2) the horizontal principal stresses increase with depth in such a way to make the possibility of strike-slip faulting likely. While it is difficult to assess whether these conditions might be met at depth, it is important to note that 1) the ~N60°E direction of maximum horizontal compression is more consistent with regional indicators, 2) near the bottom of the NPR Hole the breakouts begin to rotate back in a clockwise direction (see Fig. 11), indicating that the ~N33°E direction may be a local perturbation of the stress field. Thus, overall, the maximum horizontal stress is oriented roughly parallel to the Pen Branch Fault, indicating that it is unlikely to accomodate the reverse and strike-slip faulting characteristic of earthquakes in the southeastern U.S.

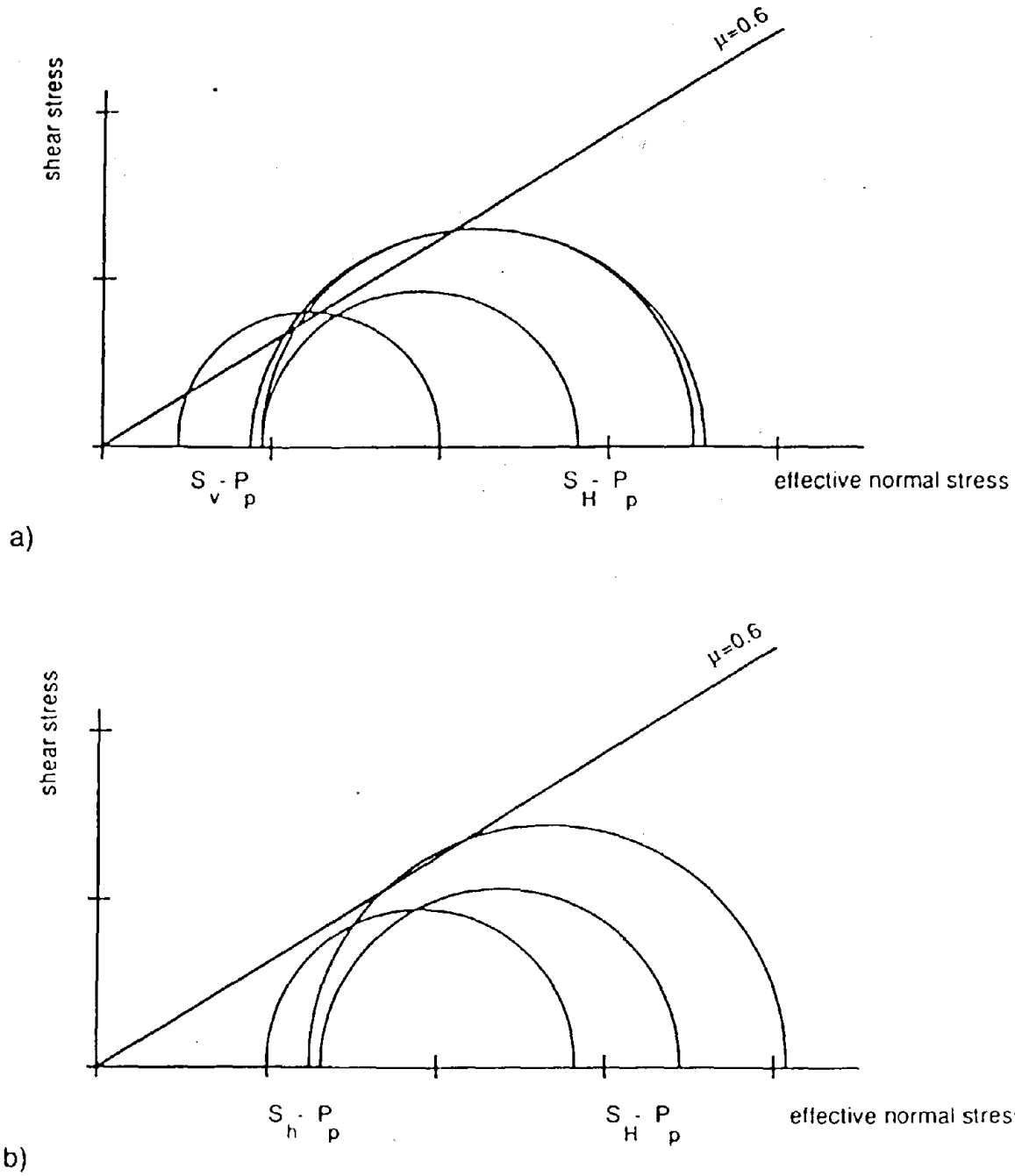

Figure 15. Mohr circle representations of stress magnitudes measured in the NPR hole. a) Data from 1100-2400' with $S_1 \equiv S_{Hmax}$, $S_2 \equiv S_{hmin}$ and $S_3 \equiv S_v$. b) Data from 2400'-3400' with $S_1 \equiv S_{Hmax}$, $S_2 \equiv S_v$ and $S_3 \equiv S_{hmin}$. Results at 2406.1 ft. are shown in both, as $S_h \approx S_v$.

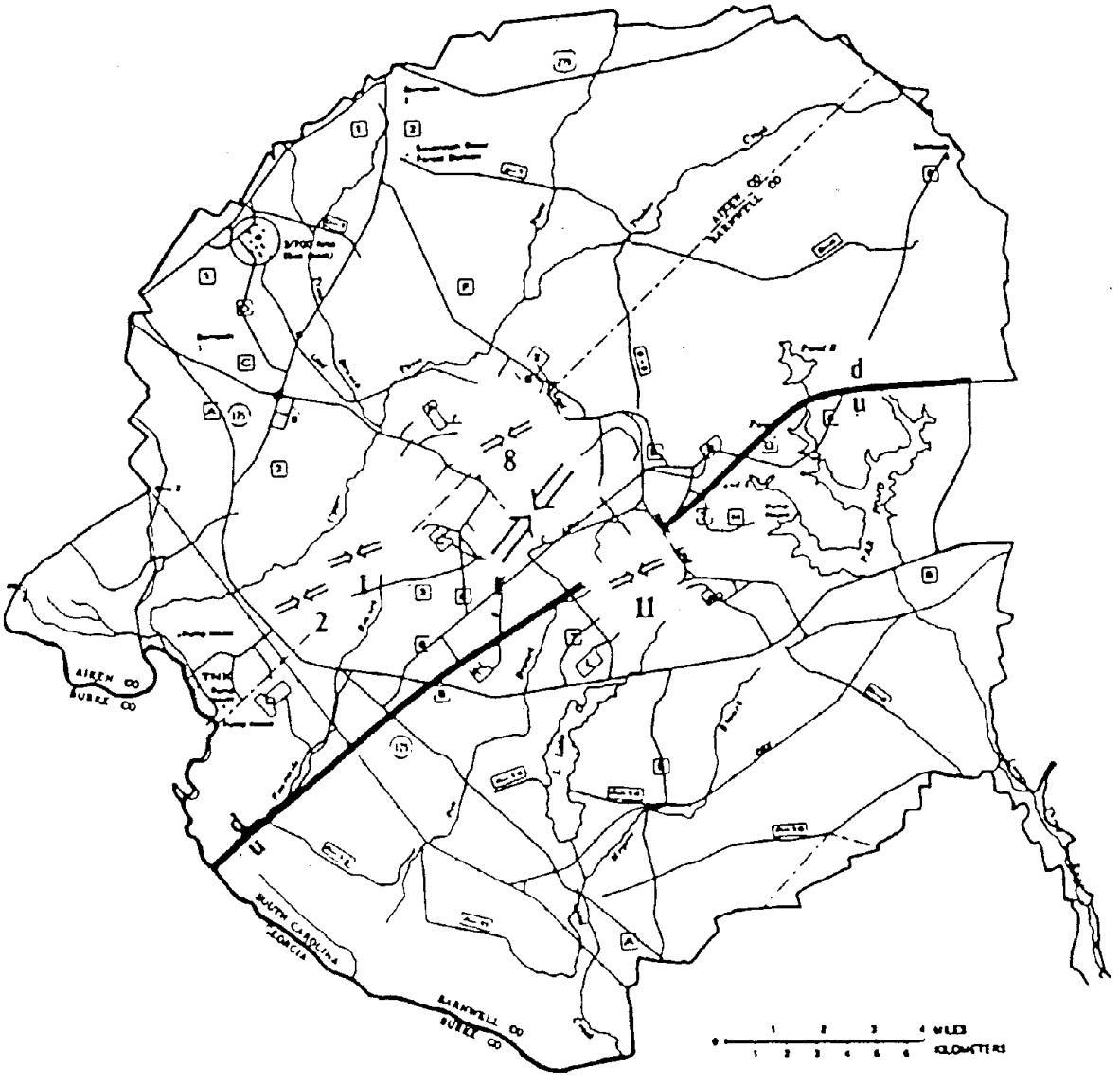

Figure 16 Map of the Savannah River Site, showing the stress orientation determinations discussed in this report. Also shown is the ~N55°E-trending Pen Branch Fault.

Conclusions

Based on in situ stress measurements over the depth interval 1200 to 3400 feet within the NPR Hole, the analysis of previous stress measurements at shallow depths at the SRS, and regional stress indicators, we find that the likelihood of reverse movement along NE trending faults like the Pen Branch is extremely small. While a reverse-faulting state was measured at depths up to 2100', the S_{Hmax} direction in that depth interval is N50-70°E, nearly parallal to the strike of the Pen Branch. The S_{Hmax} orientation at greater depth (2500-3800 feet) is N33°E (±15°), but it begins to rotate back towards a more easterly direction near the bottom of the NPR Hole (3800-4000 feet). While the horizontal stress difference between 2400' and 3400' approaches that necessary to cause strike-slip on well-oriented faults (and thus appears to be consistent with the occurrence of a very shallow (<1-km) earthquake beneath SRS in 1985 [Talwani et al., 1986]), the state of stress in this depth interval cannot be reliably extrapolated to greater depth.

Overall, the state of stress measured at the SRS seems to be consistent with similar measurements and with the seismotectonics of the southeastern US. A highly compressional stress field exists at very shallow depth which could lead to the occurrence of very shallow, very small magnitude reverse faulting earthquakes. The ENE direction of maximum horizontal compression is similar to that measured elsewhere in the region, is consistent with the focal mechanisms of compressional (strike-slip and reverse faulting) earthquakes in the southeastern US, and is as expected from the ridge-push plate driving force. In this regard, the general consistency of the data within the surrounding area and that from inside the SRS provides further evidence that compressional fault offsets along ENE striking faults like the Pen Branch would seem to be highly unlikely.

References Cited

Anderson, T.O. and E.J. Stahl, 1967. A study of induced fracturing using an instrumental approach, *J. Petrol. Technol.*, 261-267.

Anderson, R.N., and M.D. Zoback, 1989. Did surface compression arrest propagation of rupture during the Oroville 1975 normal faulting earthquake? *Scientific Drilling* , 1, 82-89.

Barton, C.A., L.G. Tesler and M.D. Zoback, 1991. Interactive image analysis of borehole televiewer data, in Automated Pattern Analysis in Petroleum Exploration, Palaz and Sengupta (Eds.), Springer-Verlag, New York, Chapter 12, 217-242.

Baumgartner, J. and M.D. Zoback, 1989. Interpretation of hydraulic fracturing pressure-time records using interactive analysis methods, Int'l. J. Rock Mech. Min. Soc., 26, 461-470.

Brace, W.F. and D.L. Kohlstedt, 1980. Limits on lithospheric stress imposed by laboratory experiments, *J. Geophys. Res.*, 85, p. 6248-6252.

Bell, J. S. and D.I. Gough, 1979. Northeast-southwest compressive stress in Alberta: Evidence from oil wells, *Earth Planet. Sci. Lett.*, 45, 475-482.

Bredehoeft, J.D., R.G. Wolff, W.S. Keys, and E. Shuter, 1976. Hydraulic fracturing to determine the regional in-situ stress field, Piceance Basin, Colorado, *Geol. Soc. Am. Bull.*, 87, 250-258.

Byerlee, J.D., 1978. Friction of rock, *Pure Appl. Geophys.*, 116, 615-626.

Coyle, B. J., M. D. Zoback, and D. Moos, 1986. In-situ stress and fracture studies in three ADCOH site survey core holes (abs.), *EOS, Trans. AGU*, (67), p. 1242.

Ebel, J.E., 1988. Comparisons of the 1981, 1982, 1986 and 1987 swarms at Moodus, Connecticut (abs), *EOS, Trans. AGU* (69), 495.

Jaeger, J.C., and N.G.W. Cook, 1969. *Fundamentals of Rock Mechanics*, Methuen and Co., Ltd., London, 515 pp.

Haimson, B. C. and C. Fairhurst, 1967. Initiation and extension of hydraulic fractures in rocks, *Soc. of Petr. Eng. Journal.*, p. 310.

Herrmann, R.B., 1986. Surface-wave studies of some South Carolina earthquakes, BSSA 67, 111-121.

Hayashi, K., and I. Sakurai, 1989. Determination of instantaneous shut-in pressures in hydraulic fracturing tectonic stress measurements, Proc. Int. HDR Geother. Energy Conf., Cornwall, 27-30 June.

Hickman, S.H. and M.D. Zoback, 1983. The interpretation of hydraulic fracturing pressure-time data for in situ stress determination, Proc. of a Workshop on Hydraulic Fracturing Stress Measurements, U.S. National Committee for Rock Mechanics, National Academy Press, p. 44-54.

Hubbert, M.K. and D.G. Willis, 1957. Mechanics of hydraulic fracturing. *J. Petrol. Technol.*, 9, p. 153-168.

Marine, I.W. and G.E. Siple, Buried Triassic basin in the central Savannah River area, South Carolina and Georgia, *Geol. Soc Am. Bull.* 85, 311-320, 1974.

Marple, R.T. and P. Talwani, The Woodstock Lineament: A possible seismogenic fault of the 1886 Charleston, South Carolina, earthquake, *Geology*, submitted, 1991.

McGarr, A., and N.C. Gay, 1978. State of stress in the earth's crust, *Ann. Rev. Earth and Planet. Sci.*, 6, 405-436.

Moos, D. and M.D. Zoback, 1990. Utilization of observations related to wellbore failure to constrain the orientation and magnitude of crustal stresses: Application to continental, DSDP and ODP boreholes, *J. Geophys. Res.*, 95, 9305-9325.

Moos, D., B. Coyle and M.D. Zoback, (in press). Physical properties and in situ stress measurements in the ADCOH Site Survey core holes, *GSA Memoirs*.

Paillet, F.L., 1991. Use of geophysical well logs in evaluating crystalline rocks for siting of radioactive-waste repositories, *The Log Analyst*, 32(2), 85-107.

Plumb, R.A. and J.W. Cox, 1987. Stress directions in eastern North America determined to 4.5 km from borehole elongation measurements, *Jour. of Geophys. Res.*,92, 4805-4816.

SAIC, 1991. Task Manual for Task 11 of Contract AA00915P, In situ stress measurements at the Savannah River Site, SAIC/SRS-01, Golden, CO.

Schmitt, D.R. and M.D. Zoback, 1989. Poroelastic effects in the determination of the maximum horizontal principal stress in hydraulic fracturing tests: A proposed breakdown equation employing a modified effective stress relation for tensile failure, *Int'l J. Rock Mech, and Mining Sci., 26,* 499-506.

Shamir, G., and M.D. Zoback, 1992. Stress orientation profile to 3.5 km depth near the San Andreas fault at Cajon Pass, California, *J. Geophys. Res.*,97, 5059-5080.

Stephannson, O. and P. Angman, 1986. Hydraulic fracturing stress measurements at Forsmark and Stidsvig, Sweden, *Bull. Geol. Soc. Finland*, 58, Pt. 1, 307-333.

Talwani, P., B.K. Rastogi, and D. Stevenson, 1980. Induced seismicity and earthquake prediction studies in South Carolina, Tenth Tech. Report to U.S. Geological Survey, contract #14-08-0001-17670.

Talwani, P.D., 1982. Internally consistent pattern of seismicity near Charleston, South Carolina, *Geology*, 10, p. 654-658.

Talwani, P., J. Rawlins, and D. Stephenson, 1986. The Savannah River Plant, South Carolina earthquake of June 9, 1985 and its tectonic setting, SSA Eastern Section meeting, (Trans.), pp. 101-106.

Zemanek, J., E.E. Glenn Jr., R.J. Norton, and R.L. Caldwell, 1970. Formation evaluation by inspection with the borehole televiewer, *Geophysics*, 35, pp. 254-269.

Zoback, M.D., J.H. Healy, J.C. Roller, G.S. Gohn, and B.B. Higgins, 1978. Normal faulting and in situ stress in the South Carolina coastal plane near Charleston, *Geology* (6), 147-152.

Zoback, M.D., H. Tsukahara, and S.H. Hickman, 1982. Stress measurements at depth within the vicinity of the San Andreas Fault: Implications for the magnitude of shear stress at depth, *J. Geophys. Res.* 85, 275-284.

Zoback, M.D., and S.H. Hickman, 1982. In situ study of the physical mechanisms controlling induced seismicity at Monticello Reservoir, S. Carolina, *J. Geophys. Res.*, 87, 6959-6974.

Zoback, M.D. and J.H. Healy, 1984. Friction, faulting, and in situ stress, *Annales Geophysicae, 2(6)*, 689-698.

Zoback, M.D., D. Moos, L. Mastin, and R.N. Anderson, 1985. Wellbore breakouts and in situ stress; *J. Geophys. Res.*, v. 90, no B7; pp. 5523-5530.

Zoback, M.D., J. Baumgartner, and D. Moos, 1988, Hydraulic fracturing stress measurements in the Moodus Research Borehole and shallow earthquakes, (abs), *EOS, Trans. AGU* (69), pp. 491-492.

Zoback, M.D., D. Moos, and D.E. Stephenson, 1989a. State of stress and the relation to tectonics in the central Savannah River area of South Carolina, in Khair, A.W. (ed.), Rock Mechanics as a Guide for Efficient Utilization of Natural Resources: Proceedings of the 30th U.S. Symposium, 553-560, Balkema, Rotterdam.

Zoback, M. L., M.D. Zoback, J. Adams, M. Assumpção, S. Bell, E.A. Bergman, P. Blümling, N.R. Brereton, D. Denham, J. Ding, K. Fuchs, N. Gay, S. Gregersen, H.K. Gupta, A. Gvishiani, K. Jacob, R. Klein, P. Knoll, M. Magee, J.L. Mercier, B.C. Müller, C. Paquin, J. Rajendran, O. Stephansson, G. Suarez, M. Suter, A. Udias, Z.H. Xu, and M. Zhizhin, Global patterns of intraplate stress: A status report on the world stress map project of the International Lithosphere Program, *Nature*, 341, 291-298, 1989b.

Zoback, M.D., and Zoback, M.L., 1991. Tectonic stress field of North America and relative plate motions, *in* Slemmons, D.B., Engdahl, E.R., Zoback, M.D., and Blackwell, D.D., eds., Neotectonics of North America: Boulder, Colorado, Geological Society of America, Decade Map Vol. 1.

Zoback, M.D., and J.H. Healy, 1992. In situ stress measurements to 3.5 km depth in the Cajon Pass Scientific Research Borehole: Implications for the mechanics of crustal faulting, J. Geophys. Res., 97, 5039-5057.